# About OMICS Group

OMICS Group International is an amalgamation of Open Access publications and worldwide international science conferences and events. Established in the year 2007 with the sole aim of making the information on Sciences and technology 'Open Access', OMICS Group publishes 400 online open access scholarly journals in all aspects of Science, Engineering, Management and Technology journals. OMICS Group has been instrumental in taking the knowledge on Science & technology to the doorsteps of ordinary men and women. Research Scholars, Students, Libraries, Educational Institutions, Research centers and the industry are main stakeholders that benefitted greatly from this knowledge dissemination. OMICS Group also organizes 300 International conferences annually across the globe, where knowledge transfer takes place through debates, round table discussions, poster presentations, workshops, symposia and exhibitions.

# About OMICS Group Conferences

OMICS Group International is a pioneer and leading science event organizer, which publishes around 400 open access journals and conducts over 300 Medical, Clinical, Engineering, Life Sciences, Pharma scientific conferences all over the globe annually with the support of more than 1000 scientific associations, 30,000 editorial board members and 3.5 million followers to its credit.

OMICS Group has organized 500 conferences, workshops and national symposiums across the major cities including San Francisco, Las Vegas, San Antonio, Omaha, Orlando, Raleigh, Santa Clara, Chicago, Philadelphia, Baltimore, United Kingdom, Valencia, Dubai, Beijing, Hyderabad, Bengaluru and Mumbai.

# Magnetic Nanoparticles-based Microfludic Sensing System for Genotyping, CTC Measurement and Therapeutic Monitoring

Daxiang Cui

**Institute of Nano Biomedicine and Engineering**

**Research Institute forTranslational Medicine**

2014-8-15

上海交通大學
Shanghai Jiao Tong University

# Outline

- Current status and scientific problem of gastric cancer
- Biomarkers associated with gastric cancer
- Nano devices for ultrasenstive detection of gastric cancer biomarkers
- Multifunctional nanoprobes for Targeted Imaging and simultaneous therapy of Gastric Cancer
- Biosafety of nanoprobes
- Summary and Acknowledgement

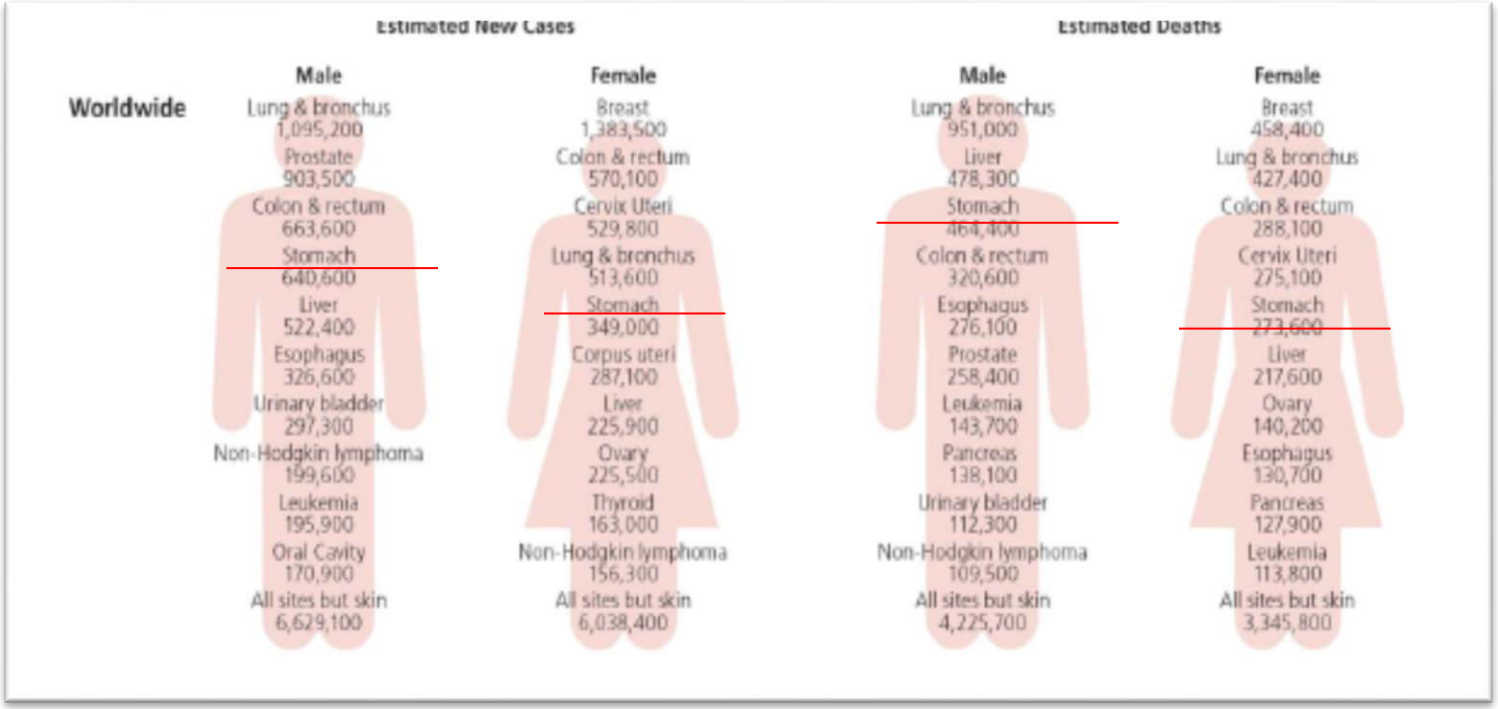
# World Cancer Distribution

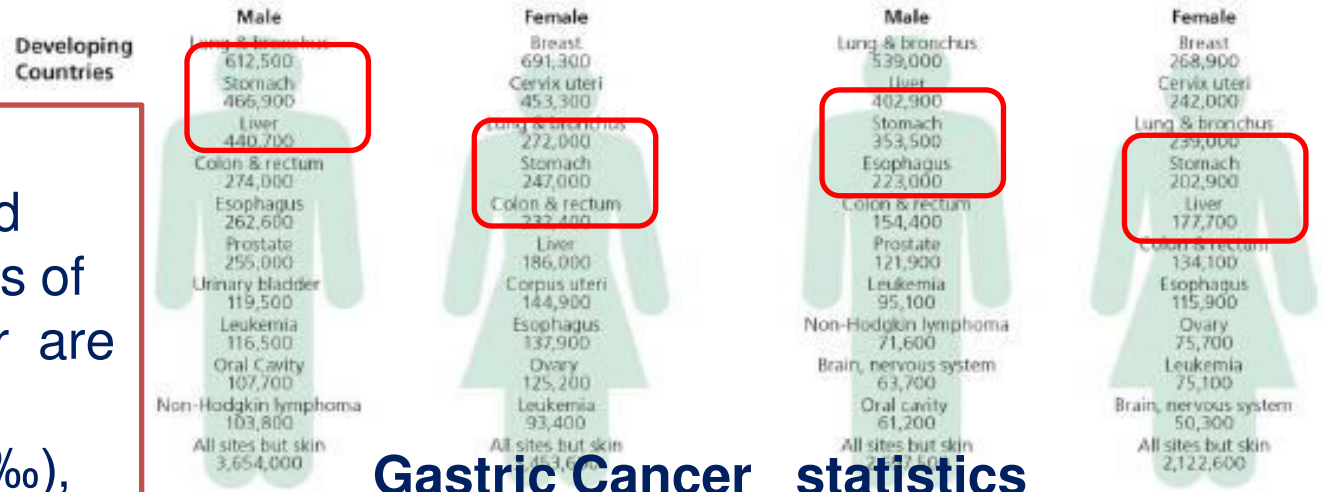



1 Eastern Africa
2 Middle Africa
3 Northern Africa
4 Southern Africa
5 Western Africa
6 Caribbean
7 Central America
8 South America
9 Northern America
10 Eastern Asia
10a Japan
10b Other E. Asia (China, Korea and Mongolia)
11 South-Eastern Asia
12 South-Central Asia
13 Western Asia
14 Central and Eastern Europe
15 Northern Europe
16 Southern Europe
17 Western Europe
18 Australia/New Zealand
19 Melanesia
20 Micronesia/Polynesia

Global Cancer Statistics

In 2008, cancer patients reached to 1.27 million
In 2020, cancer number will be 1.500 million



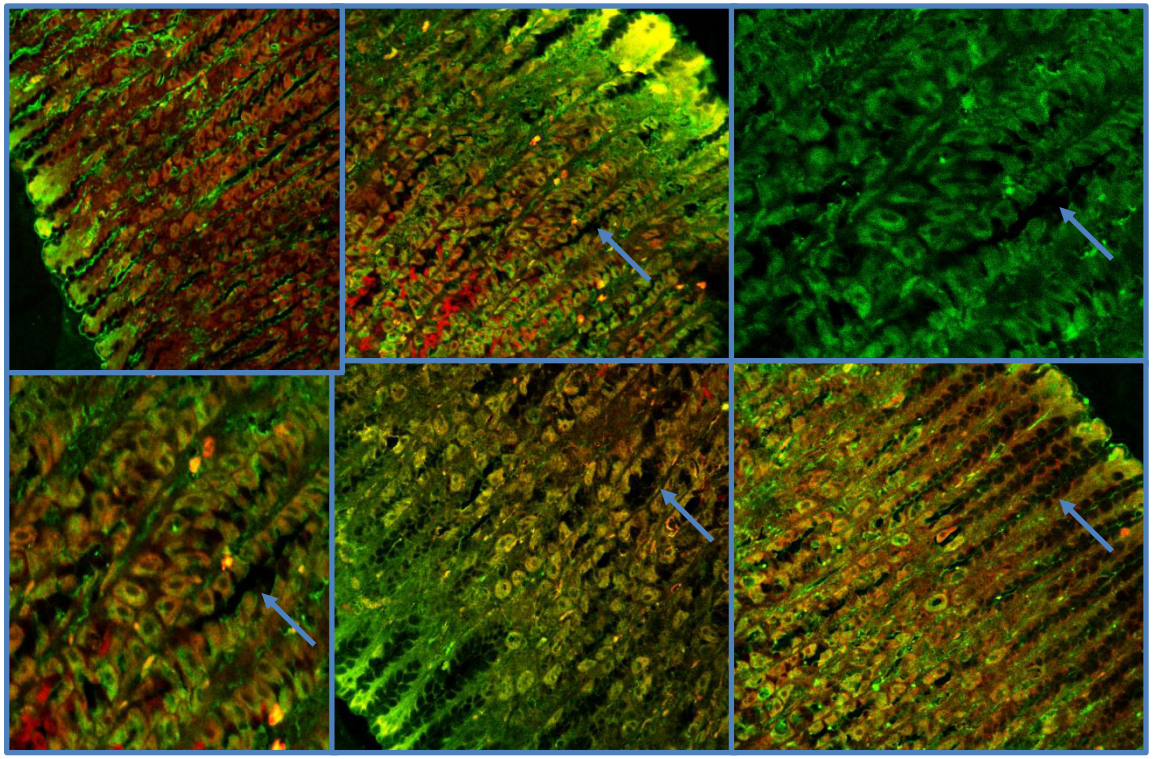



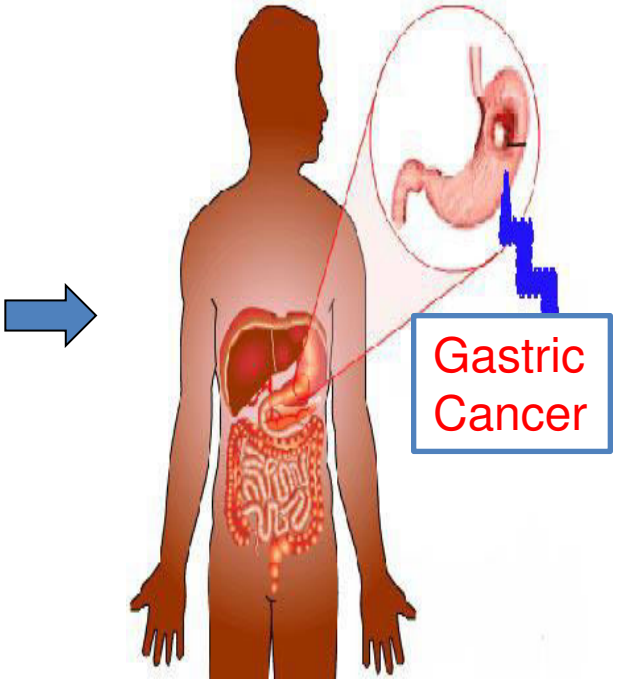

In China, incidence and mortality rates of gastric cancer are respectively second (16.7‰), third (10.4‰)

**Gastric Cancer statistics**

**CA CANCER J CLIN 2011;61:69–90.**

# From Precancerous Lesions to Gastric Cancer



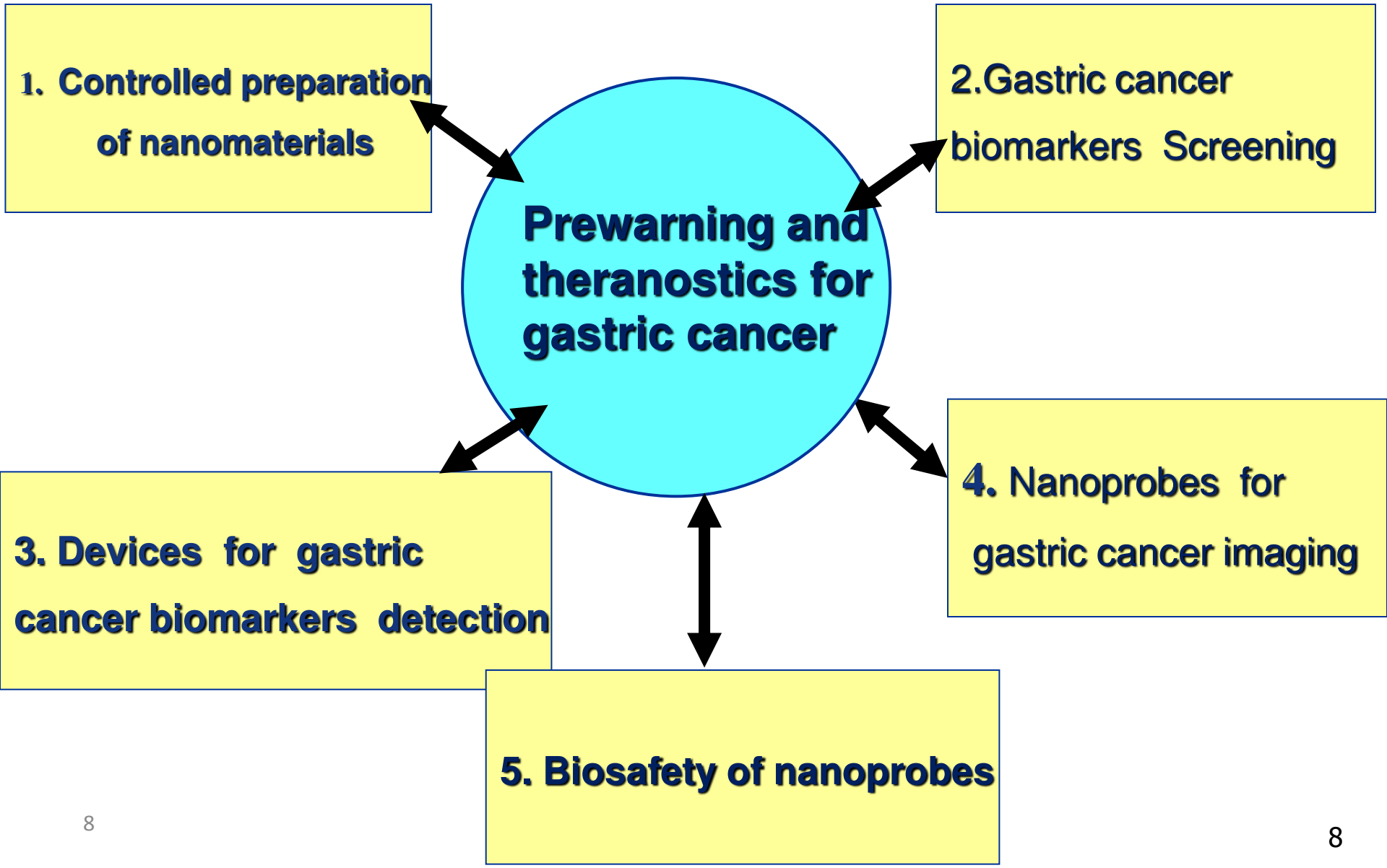



precancerous lesions

QDs-labeled MUC1 antibody
Qds-labeled HAI-178

***Ho w to find early gastric cancer ?***

# How to find early gastric cancer

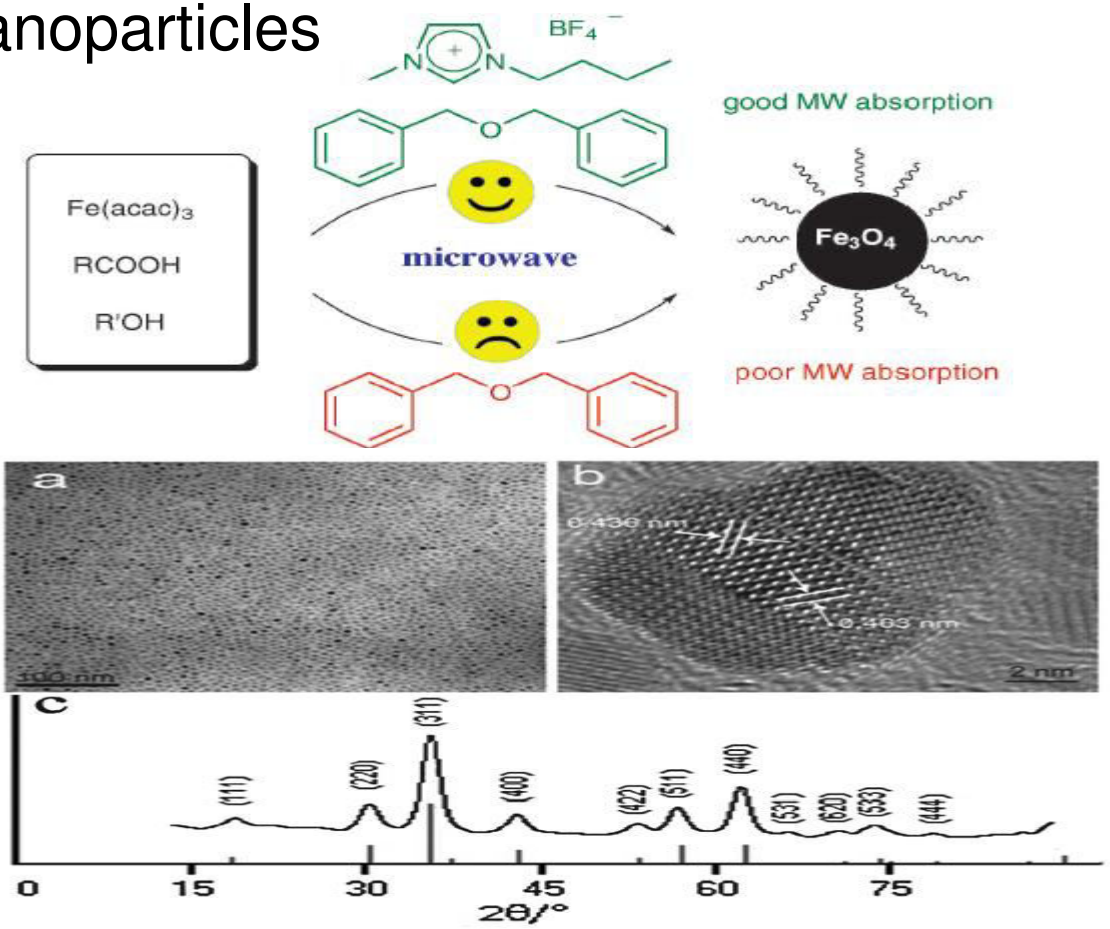





8

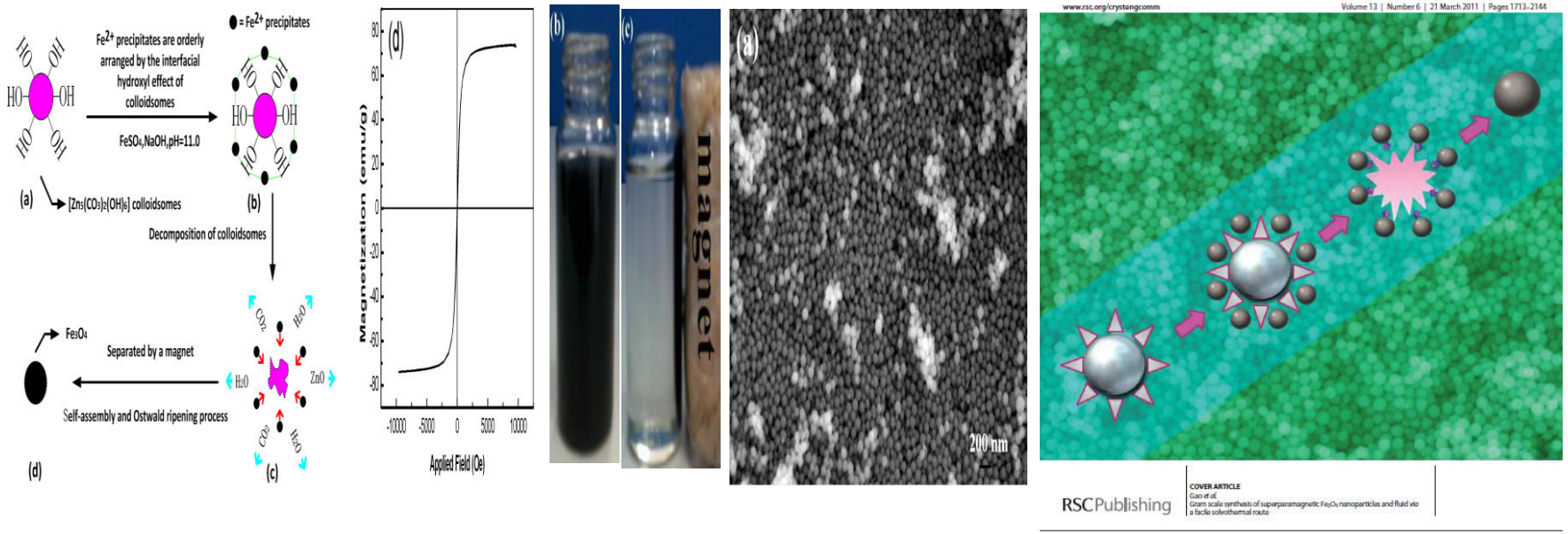
# Controlled Preparation of Nanoparticles

Magnetic nanoparticles preparation



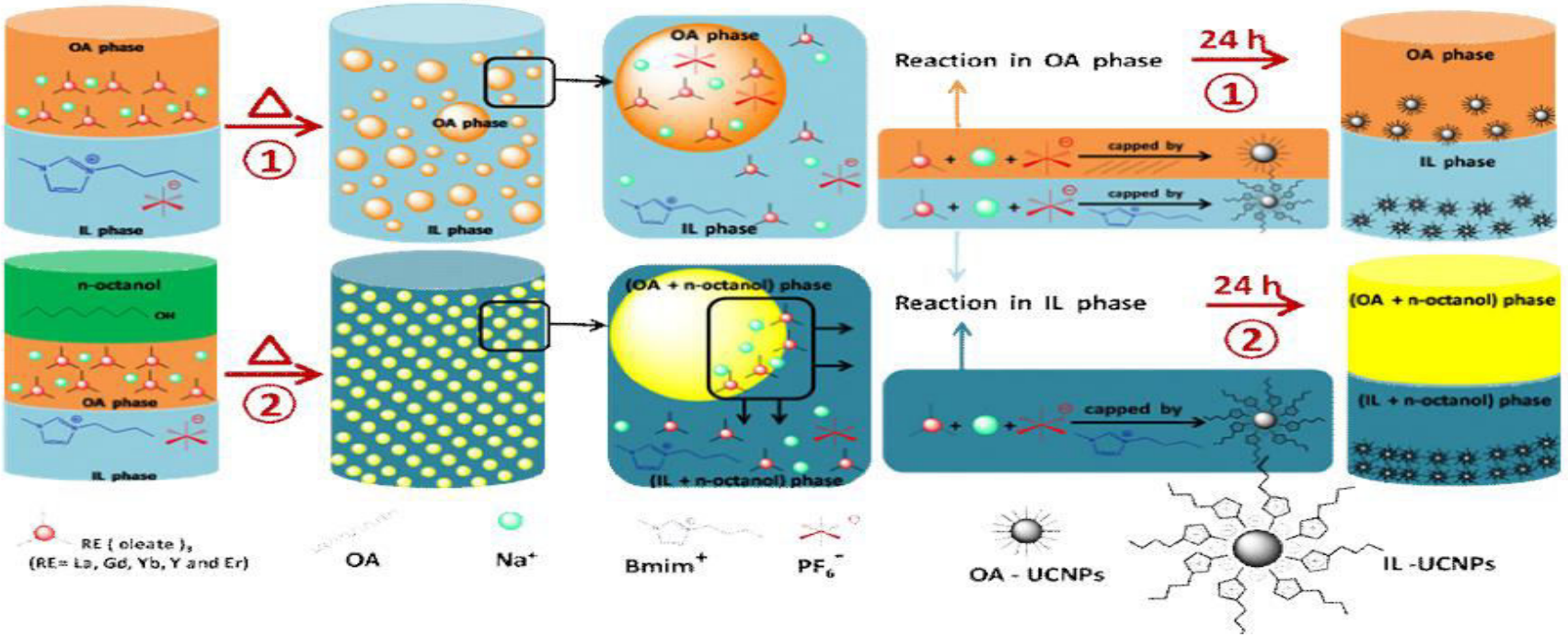

*Hu, et al. Chem. Comm. 2010; 46:3866-3868.*

# Scale preparation of magnetic nanoparticles




Gao, et al. Gram scale synthesis of superparamagnetic $Fe_3O_4$ nanoparticles and fluid via a facile solvothermal route. ***Cryst. Eng. Com.*** 2011;13:1782-1785.

# Dual Phase-Controlled Synthesis of Uniform Lanthanide-Doped Upconversion Nanocrystals Via an OA/Ionic Liquid Two-Phase System




NaGdF4: Yb, Er


He, et al. *Chem. Comm. 2011;47: 9510-9517.*

*He, et al.* Advanced Functional Materials 2011; 21:4470-4477.

He, et al. *Chem. A Europ. Journal* 2012: 18:5954-5960.

# Gastric Cancer Biomarkers Screening

VOC biomarkers

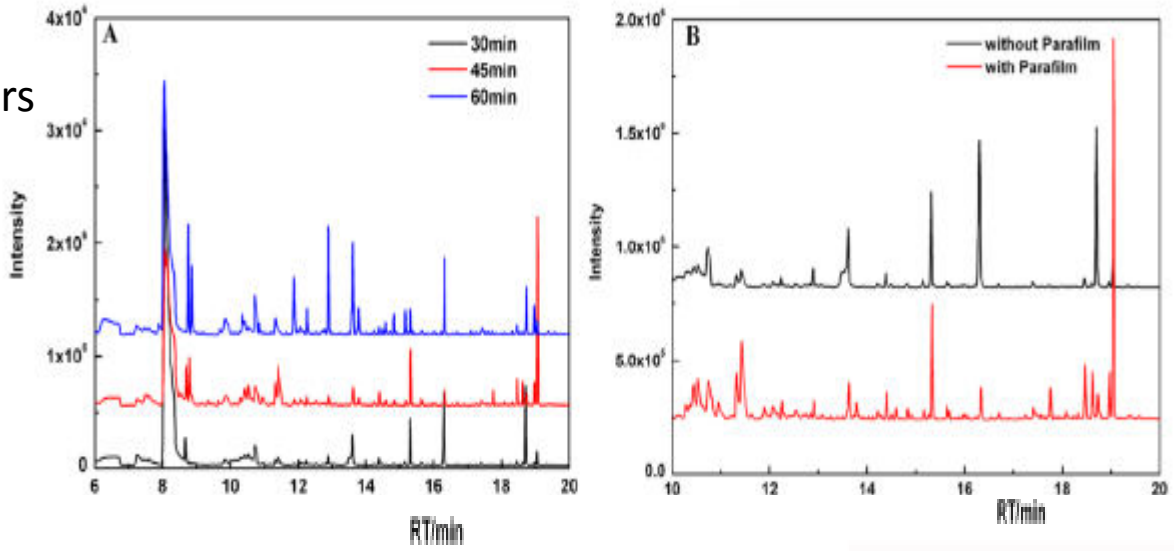



**Figure 1.** The patterns from the chromatogram of VOCs from MGC-803 gastric cancer cells that were influenced by: (A) headspace extraction time; (B) MGC-803 cells cultured with and without Parafilm

**Table 1.** Summary of different VOCs between MGC-803 cells and GES-1 cells.

| Peak | RT | Compounds | GES-1 | MGC-803 |
|---|---|---|---|---|
| 1 | 9.1 | Formic acid propyl ester | + | - |
| 2 | 10.4 | 3-octanone | - | + |
| 3 | 10.8 | 1.4-butanediol | + | - |
| 4 | 11.6 | 4-Isopropoxybutanol | ++ | + |
| 5 | 12.75 | nonanol | ++ | + |
| 6 | 18.08 | Butanone | - | + |
| 7 | 18.32 | 1-butanol,4-butoxy | ++ | + |
| 8 | 18.84 | Dodecane, 2,6,11-trimethyl | + | - |

Notes: +: VOCs present; -: VOCs absent; different numbers of + stands for different concentrations.

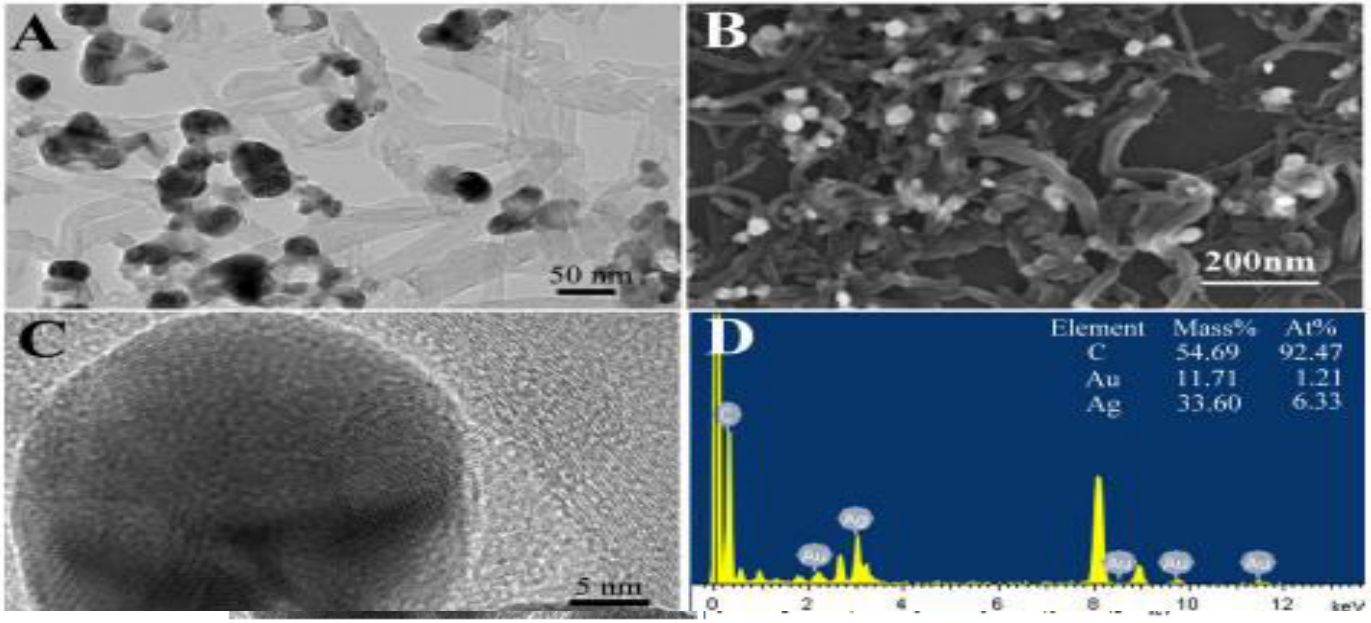



**Figure 3.** Characterization of MWNTs covered with Au-Ag nanoparticles: (A) TEM image; (B) SEM image; (C) HR-TEM image of Au-Ag nanoparticles on the surface of MWNTs; (D) the corresponding EDX spectra of MWNTs/Au-Ag nanoparticles.

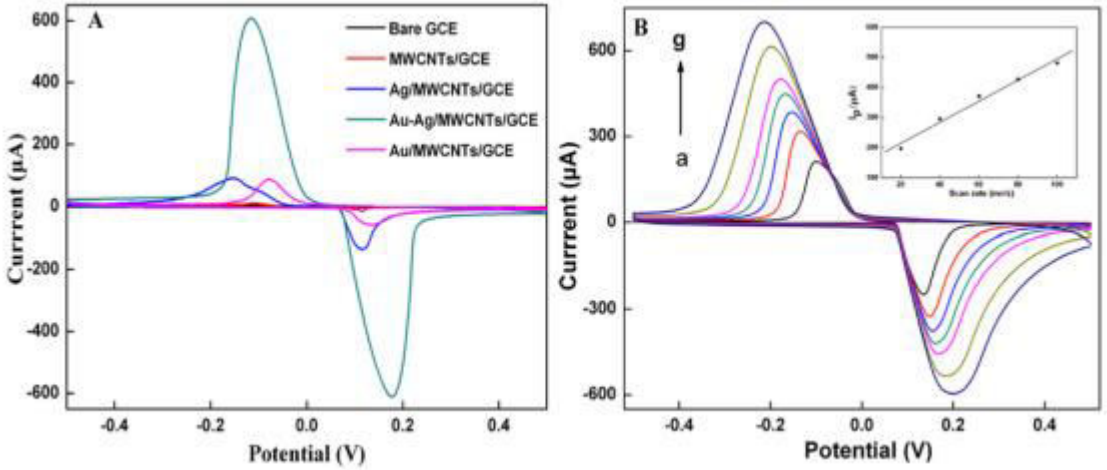



**Figure 4.** (A) Cyclic voltammograms of MWNTs/Au-Ag/GCE, MWNTs/GCE, MWNTs/Ag/GCE, MWNTs/Au/GCE and bare GCE in 0.1 M KCl solution. (B) Cyclic voltammograms of MWNTs/Au-Ag/GCE in 0.1 M KCl solution with various scan rates (from a to g: 20,40,60,80,100,150 and 200, respectively). The inset is the linear plot between the anodic peak current and the scan rate.

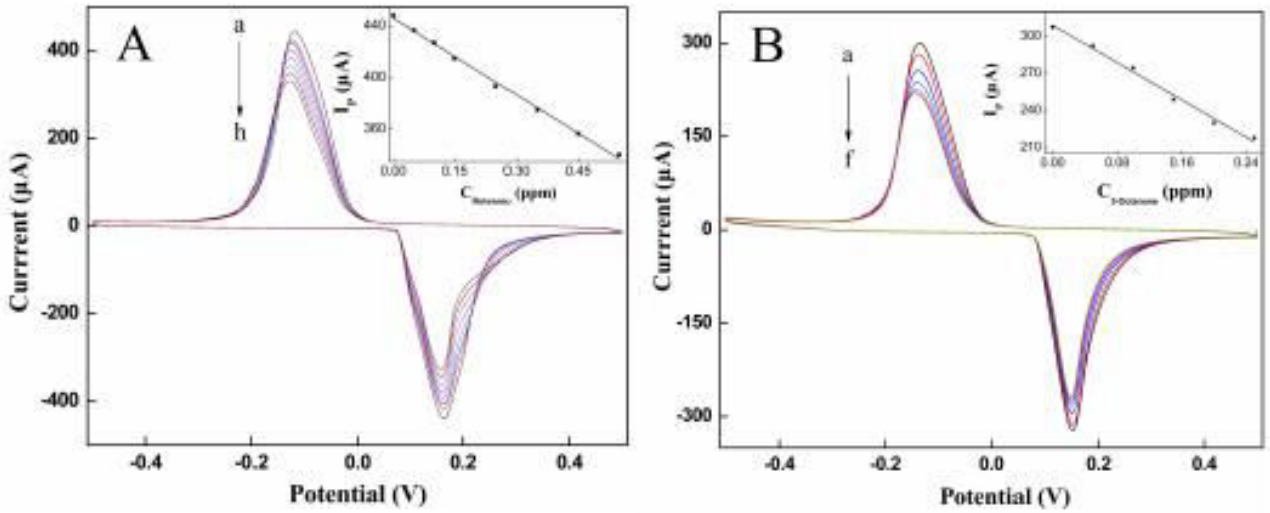



**Figure 5.** (A): The cyclic voltammograms of MWNTs/Au-Ag/GCE were exposed to different concentrations of butanone (from a to h: 0, 0.05, 0.1, 0.15, 0.25, 0.35, 0.45 and 0.55 ppm, respectively). The inset shows a line plot of the peak current ($I_p$) against concentration of butanone. (B): The cyclic voltammograms of MWNTs/Au-Ag/GCE were exposed to different concentrations of 3-octanone (from a to f: 0, 0.05, 0.1, 0.15, 0.2 and 0.25 ppm, respectively). The inset shows a line plot of the peak current ($I_p$) against concentration of 3-octanone. All the potentials are given versus SCE.

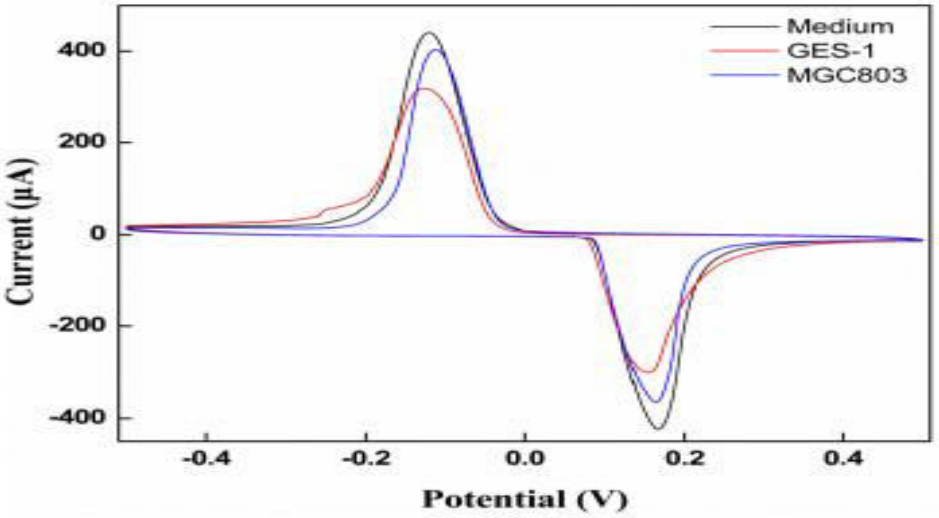
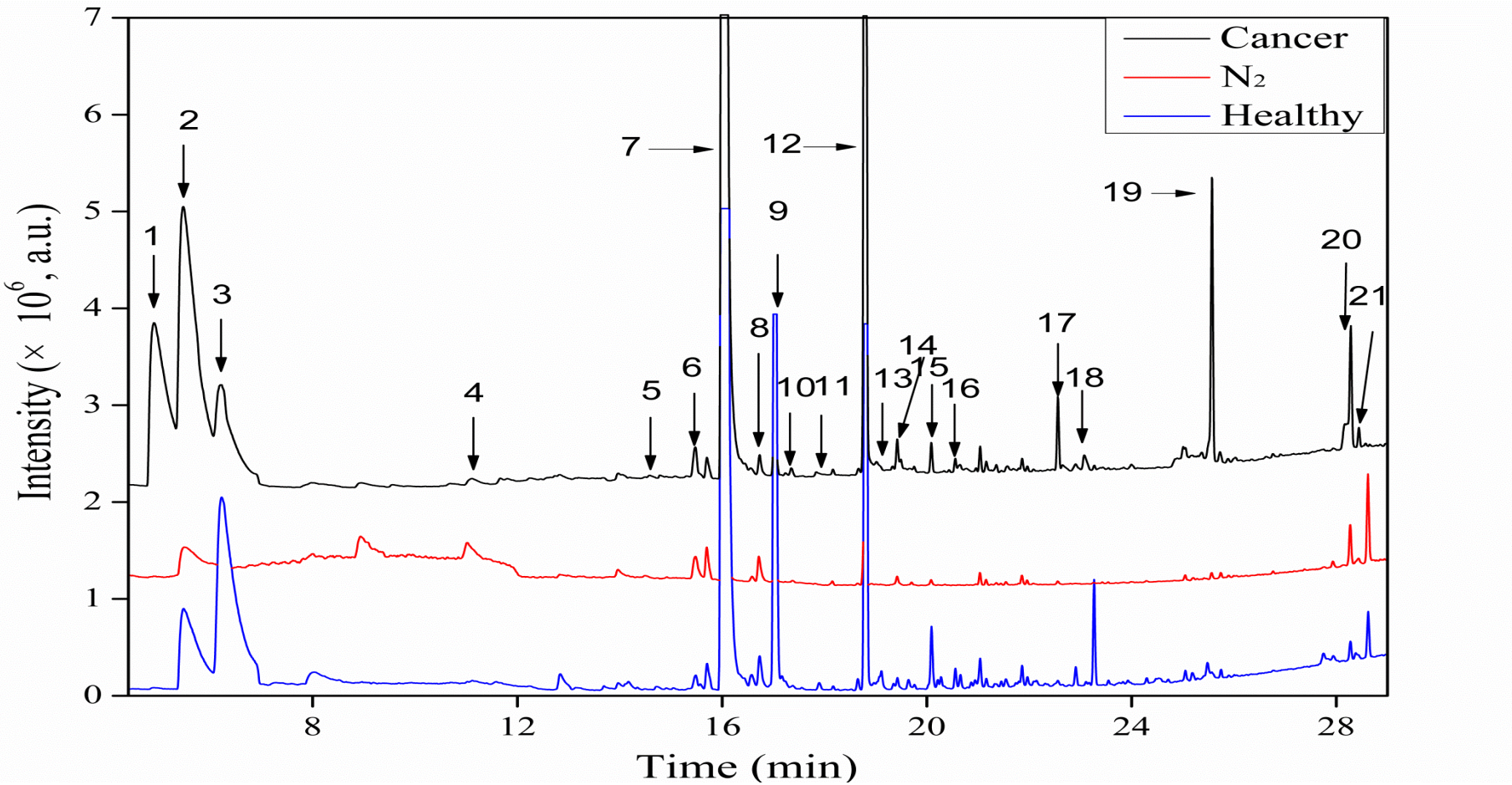



**Figure 6.** Cyclic voltammograms of MWNTs/Au-Ag/GCE was exposed to the head space of cell-free medium, MGC-803 gastric cancer cells, and GES-1 gastric mucosa cells.

Zhang, et al. Theranostics 2012; 4:152-164.

# VOC difference between healthy people and patients with gastric cancer



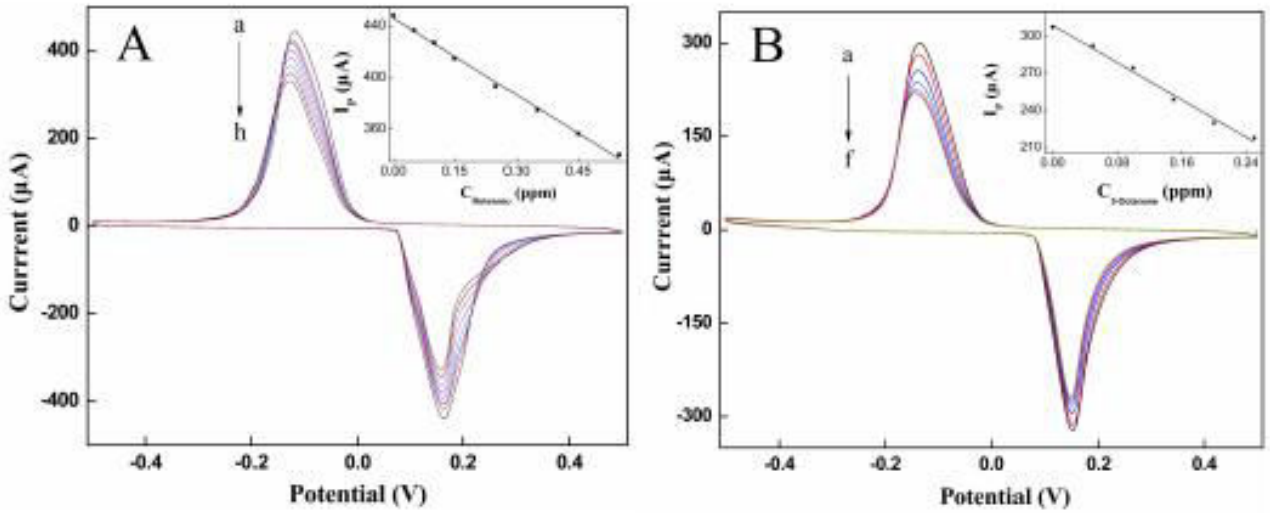



**Figure 5.** (A): The cyclic voltammograms of MWNTs/Au-Ag/GCE were exposed to different concentrations of butanone (from a to h: 0, 0.05, 0.1, 0.15, 0.25, 0.35, 0.45 and 0.55 ppm, respectively). The inset shows a line plot of the peak current ($I_p$) against concentration of butanone. (B): The cyclic voltammograms of MWNTs/Au-Ag/GCE were exposed to different concentrations of 3-octanone (from a to f: 0, 0.05, 0.1, 0.15, 0.2 and 0.25 ppm, respectively). The inset shows a line plot of the peak current ($I_p$) against concentration of 3-octanone. All the potentials are given versus SCE.

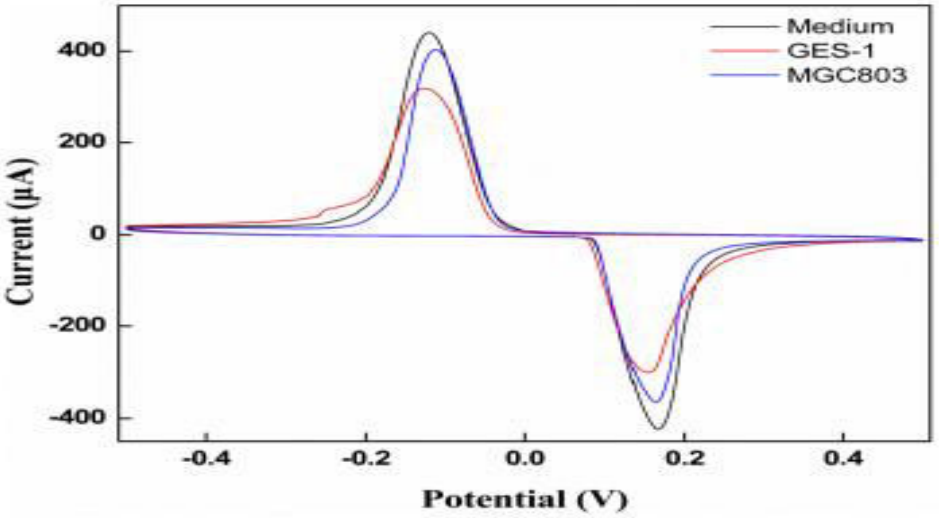
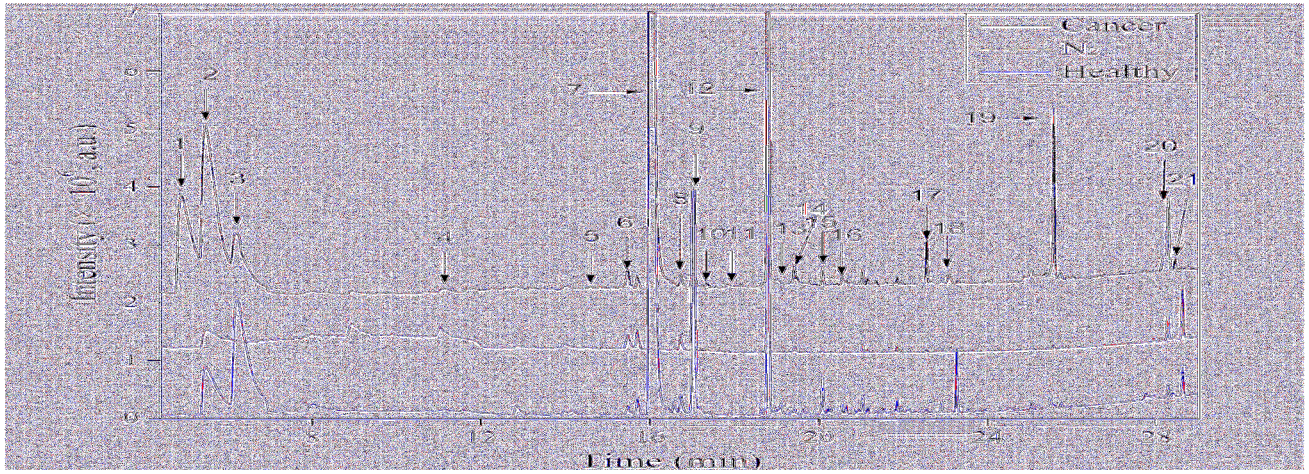
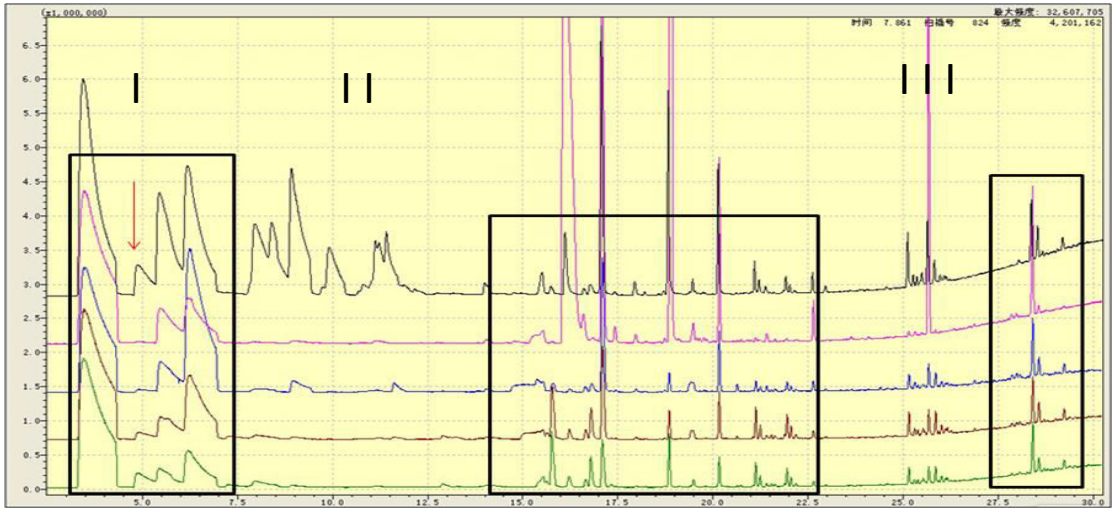



**Figure 6.** Cyclic voltammograms of MWNTs/Au-Ag/GCE was exposed to the head space of cell-free medium, MGC-803 gastric cancer cells, and GES-1 gastric mucosa cells.

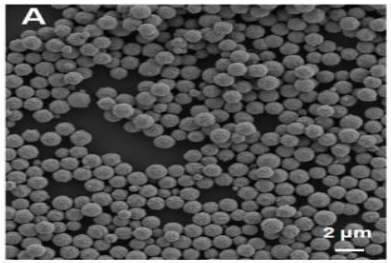
Zhang, et al. Theranostics 2012; 4:152-164.

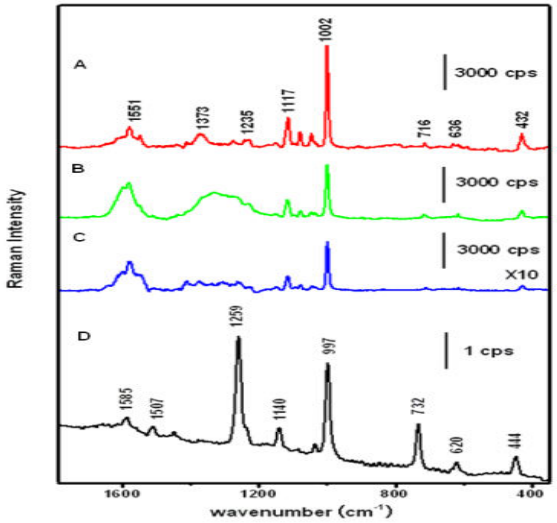
# VOC difference between healthy people and patients with gastric cancer



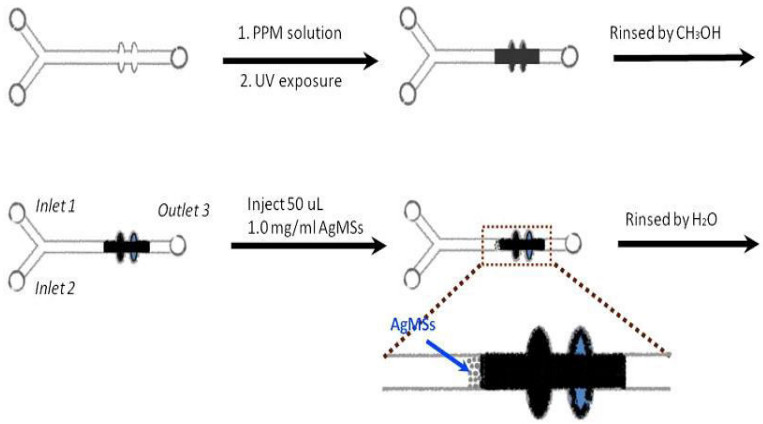

**Three area at RT： 2-7min，15-22min，24-30min**

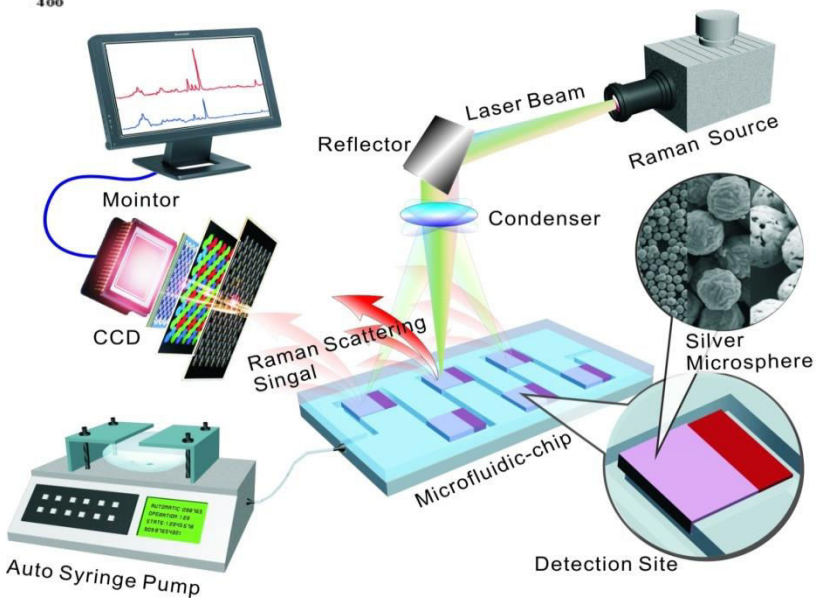



- 以乳酸菌作模板，首次可控制备空心银微球
- 灵敏度：$10^{-15}$ M 拉曼分子, 增强系数：$10^{11}$倍
- Yang, et al. Green Chem. 2010;12:2038-2042.

  发明专利授权：ZL201010257653.X




制备含有空心银微球的整体柱

将气体分子富集于检测区域



阿尔贝·费尔 与彼得·格林贝格尔

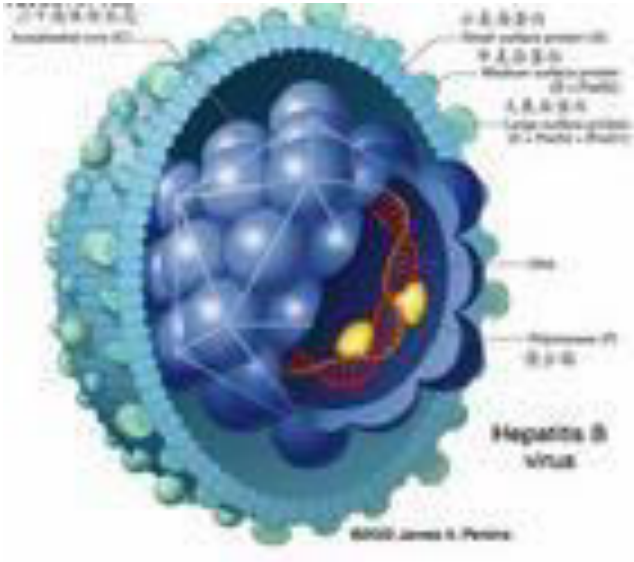
Obtain 2007 Nobel Physcis Prize for finding Giant MagnetoResistance (GMR)

# 病毒基因快速分型的微流控GMR传感器

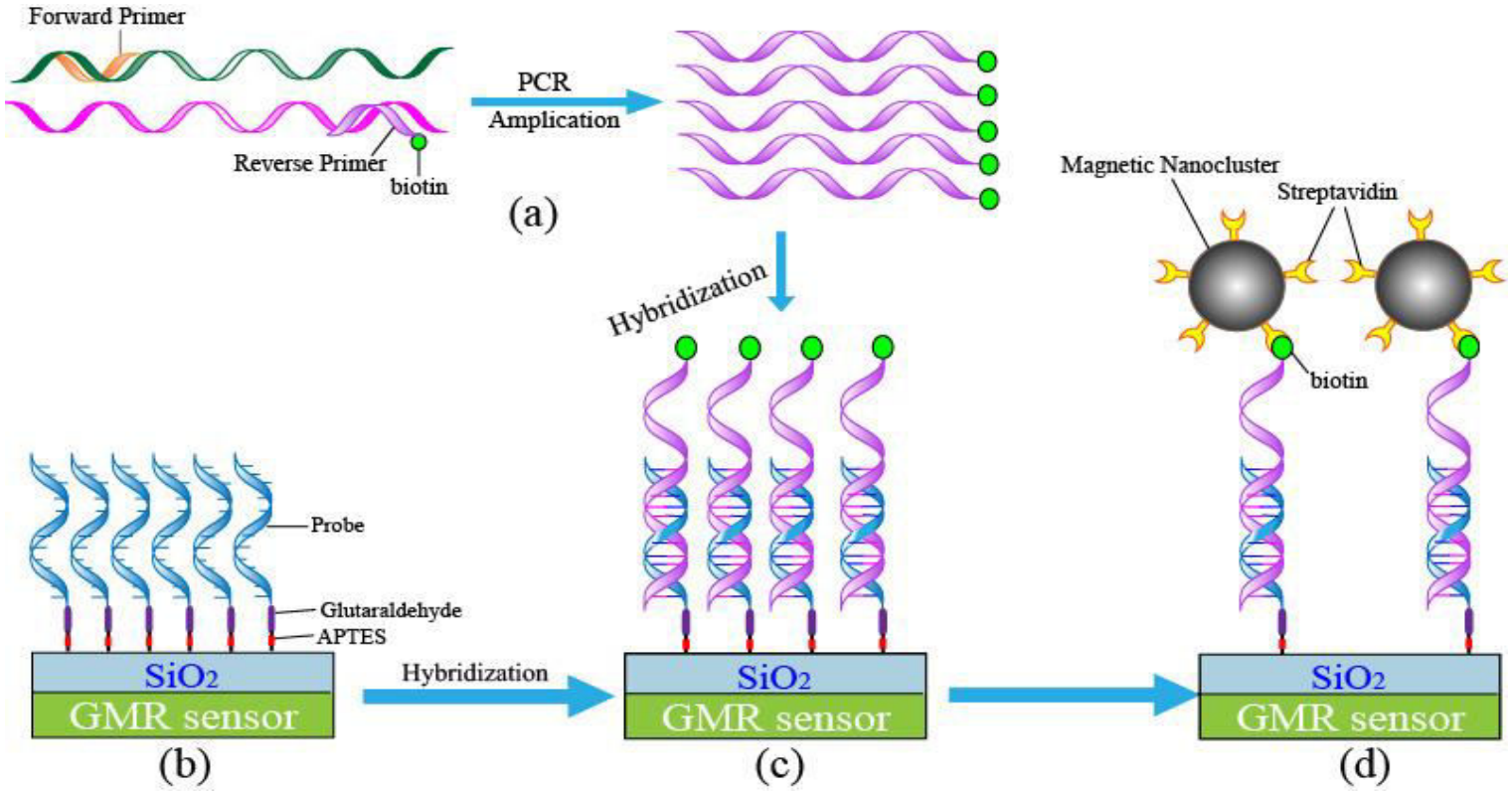
HBV epidemiol characterization：

Liver cancer:
20 billion
3.5 billion with HBV virus
China:
7.18% population with HBsAg

Gene types:
A to I
In china, A,B,C,D four types
B type: 41%; C type: 53%




HBV virus structure




Schematic of detection principle

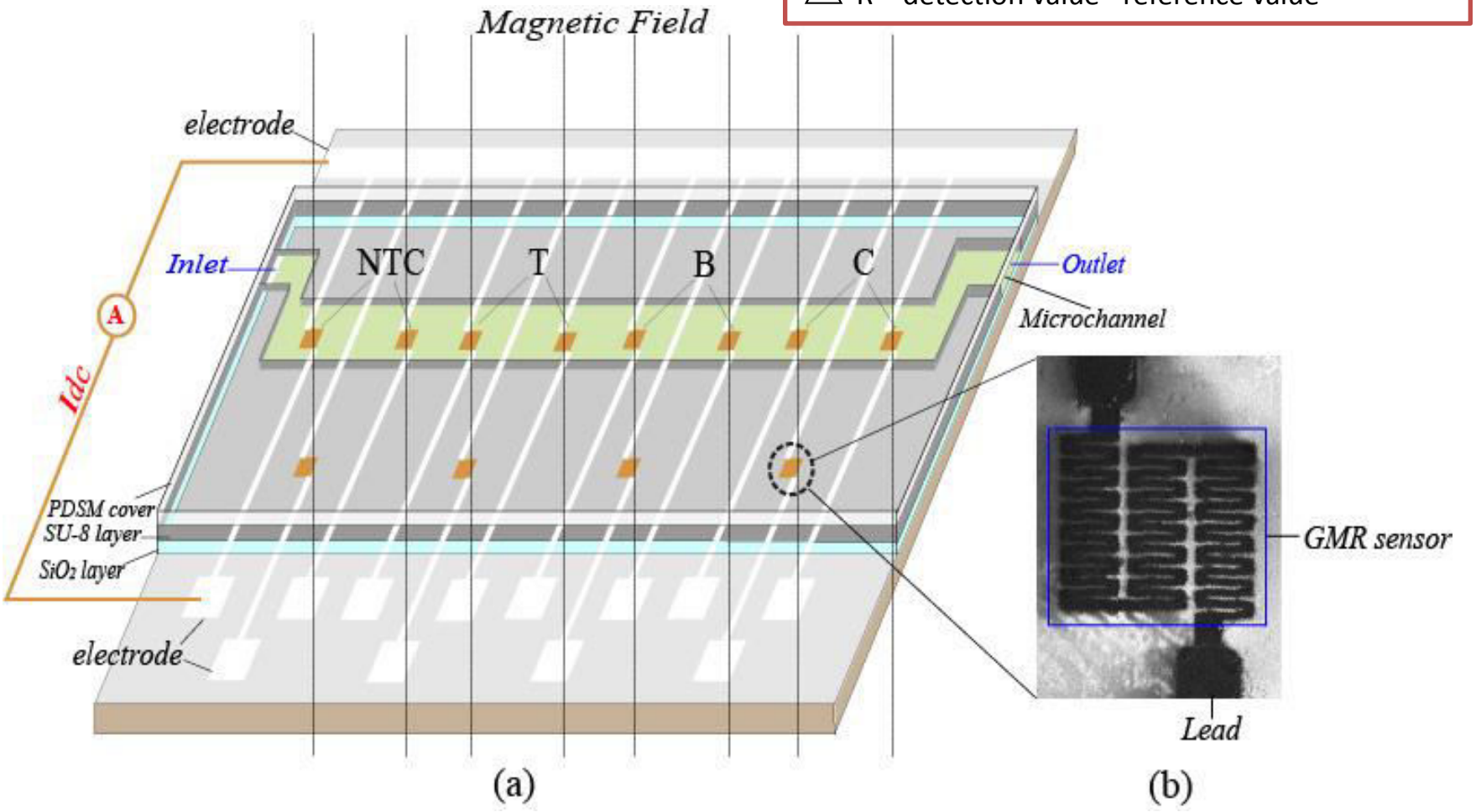
(a) amplication of target DNA by PCR;
(b) immobilization of the probe DNA;
(c) hybridization of the analyte DNA;
(d) binding of the magnetic microspheres.

# GMR sensing chip

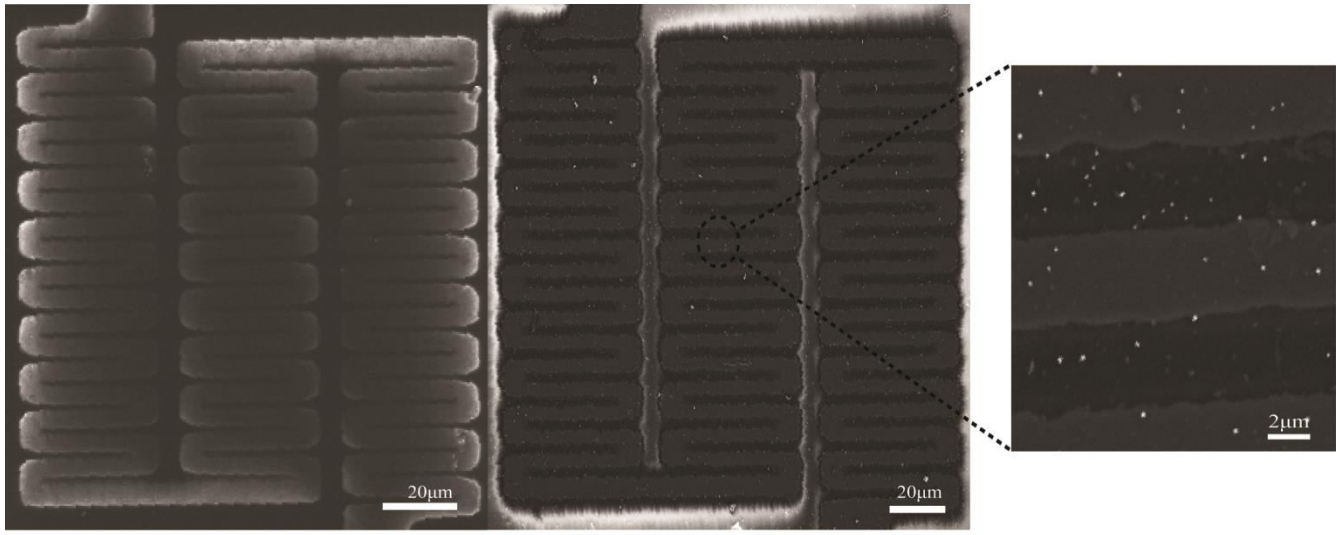
B or C

T

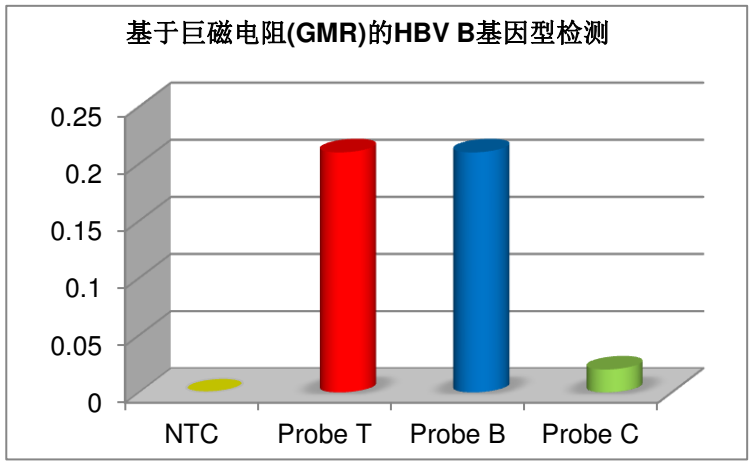
△ R = detection value –reference value

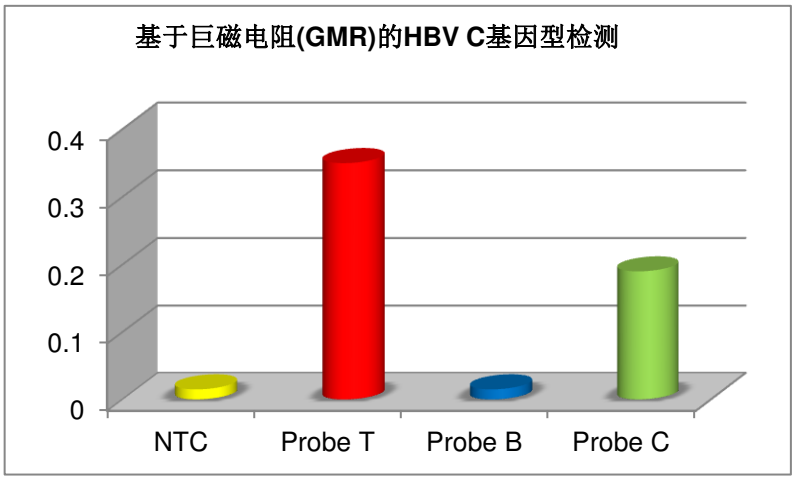



**Conformation of the magnetoresistive biochip: (a) fabrication of the biochip; (b) pattern of the GMR sensor**




SEM images of negative and positive regions of GMR biochip



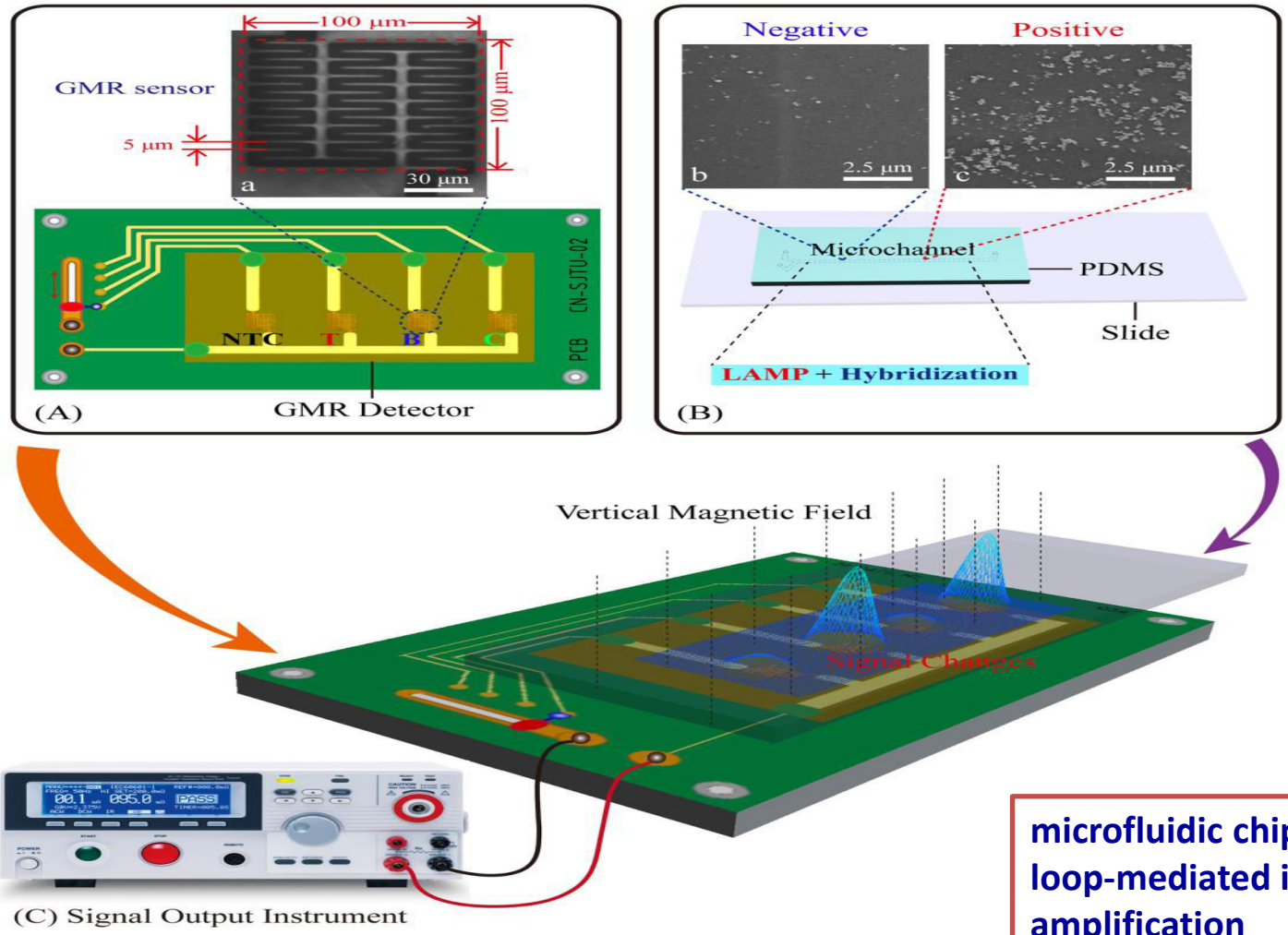



# GMR changes of different genotypes （n =4, X ±SE）

| Genotype samples | | Signal change, in mΩ(positive signals in bold) | | | |
|---|---|---|---|---|---|
| | | NTC region | T region | B region | C region |
| Genotype B | Reference | | 32.50±5.90 | | |
| | Detection | 42.50±8.54 | 262.50±27.80 | 262.50±14.93 | 47.50±8.54 |
| | Net value | 10.00±2.64 | **230.00±21.90** | **230.00±9.03** | 15.00±2.64 |
| Genotype C | Reference | | 28.75±3.50 | | |
| | Detection | 42.50±11.08 | 272.50±27.80 | 52.50±4.79 | 203.75±15.19 |
| | Net value | 13.75±7.58 | **243.75±24.30** | 23.75±1.29 | **175.00±11.69** |

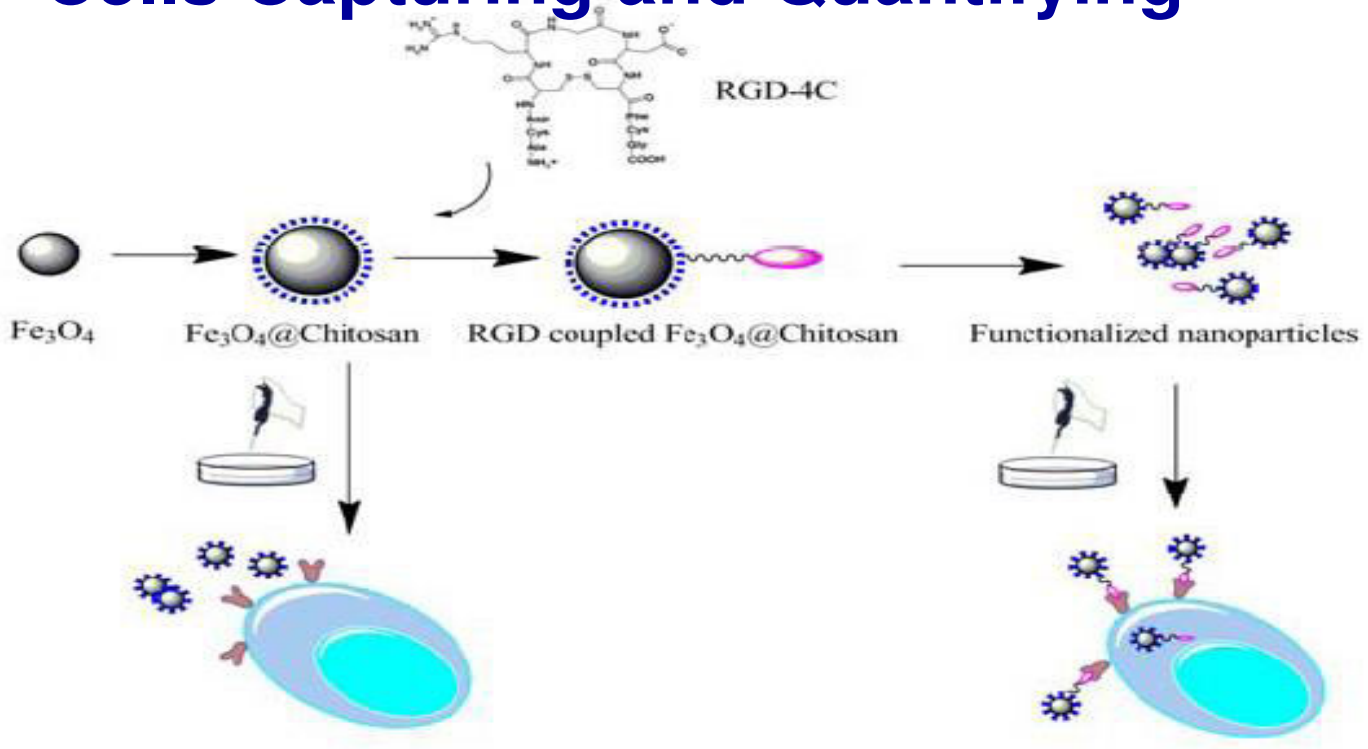
**sensitivity： HBV DNA real time PCR level**

Xiao Zhi, et al. Quick genotyping detection and line probe ofHBV by giant magnetoresistive biochip combined with PCR and line probe assay***. Lab-on a chip 2012; 12:741-745.***



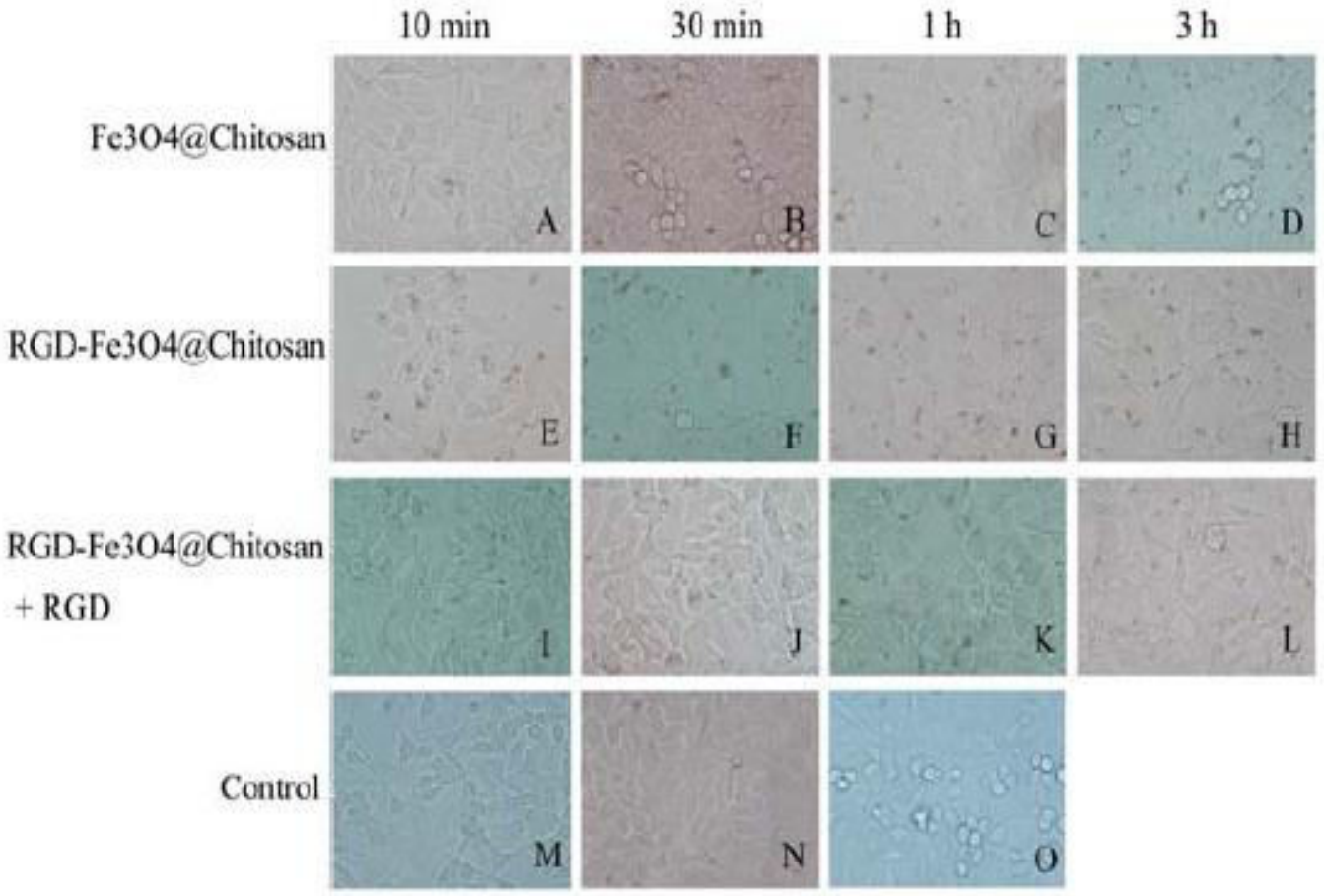

microfluidic chip
loop-mediated isothermal amplification
GMR sensor

# GMI Sensing System for Gastric Cancer Cells Capturing and Quantifying




biomarker：RGD-4C
Chitosan modified magnetic nanoparticles
RGD peptide conjugated with magnetic nanoparticles
Capture cancer cells

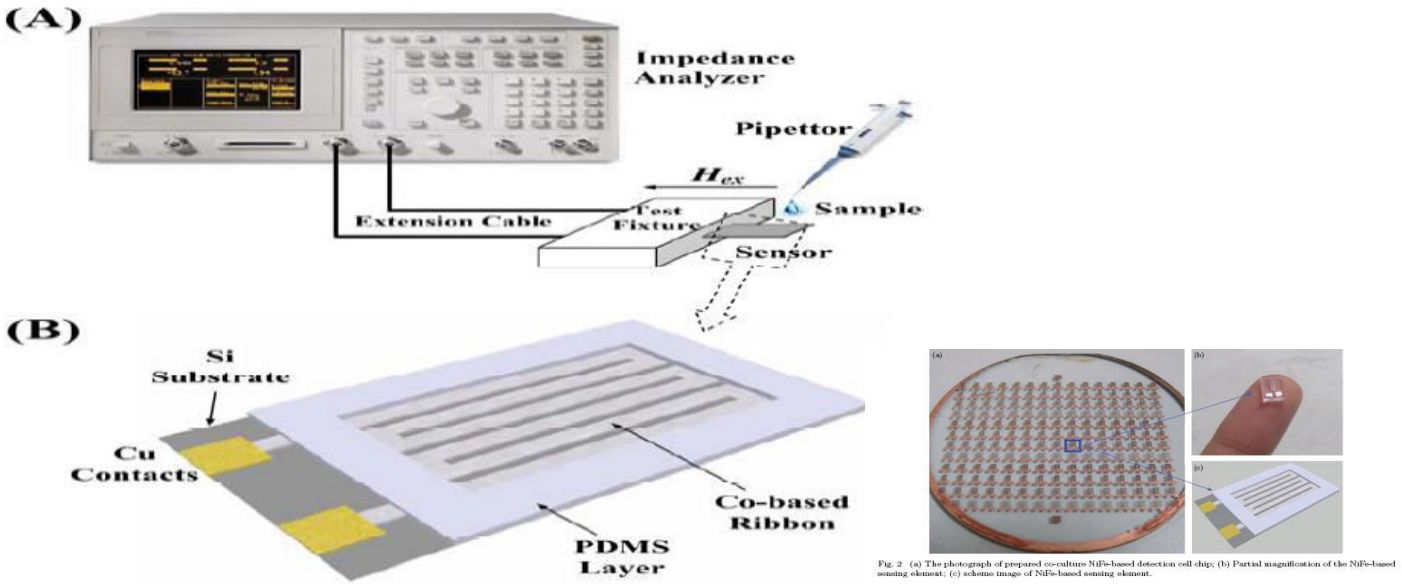
Chen, et al. Biosensors and Bioelectronics 2011:6:2435-2442.



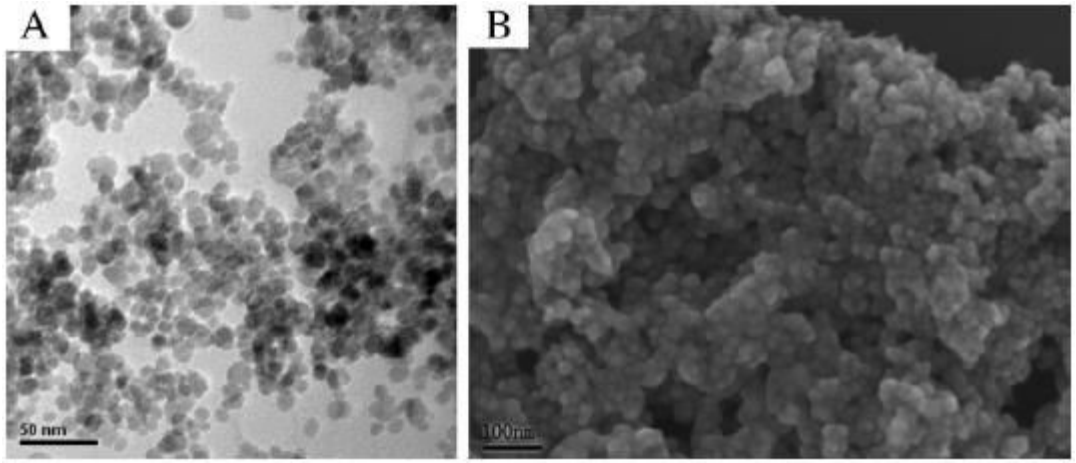

Endocytosis of functionalized magnetic nanoparticles，

E,F,G,H: functionalized NPs enhanced absorption，

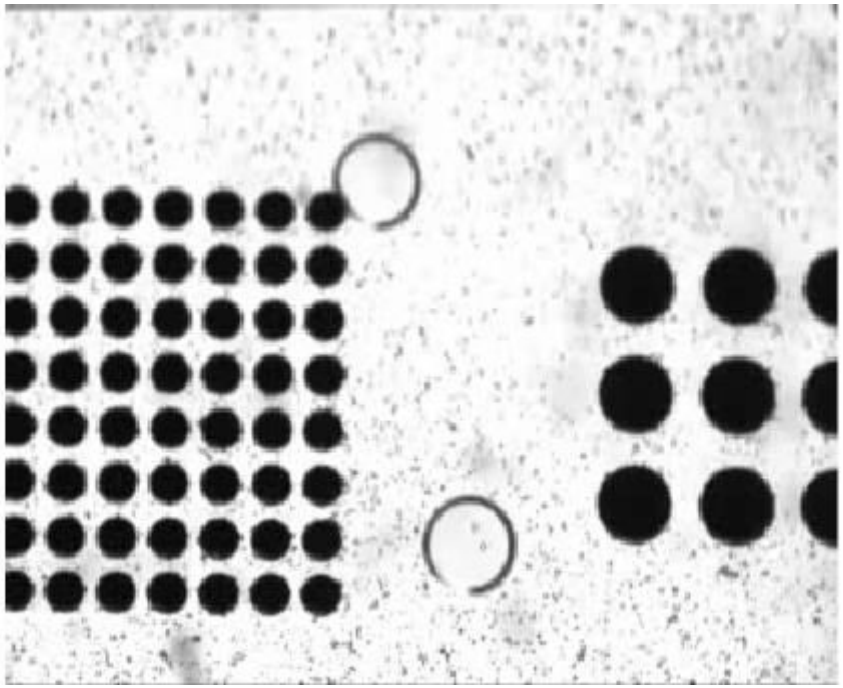
(A,B,C,D),L ,I,J,K,L : competing inhibition， Control o: MGC803 cells



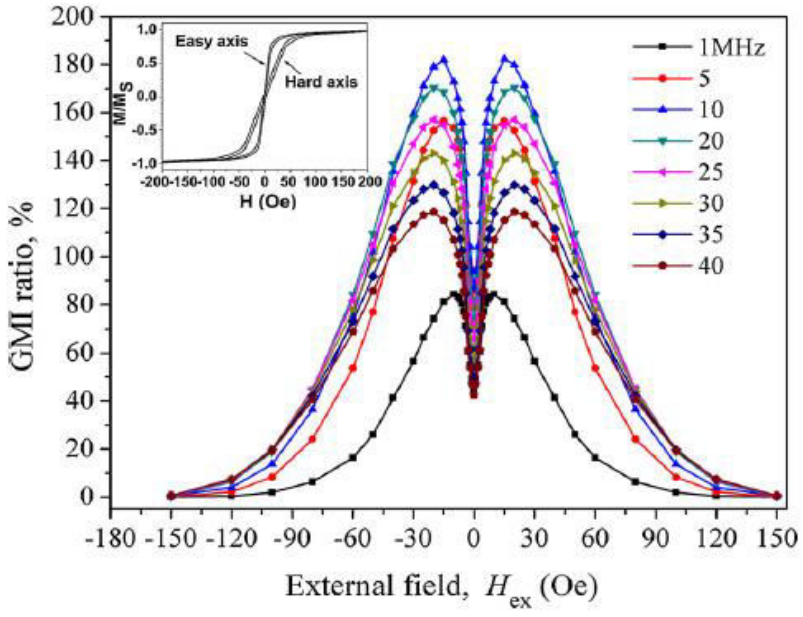

GMI sensor detection system:
(A) sensing system; (B)GMI sensing element

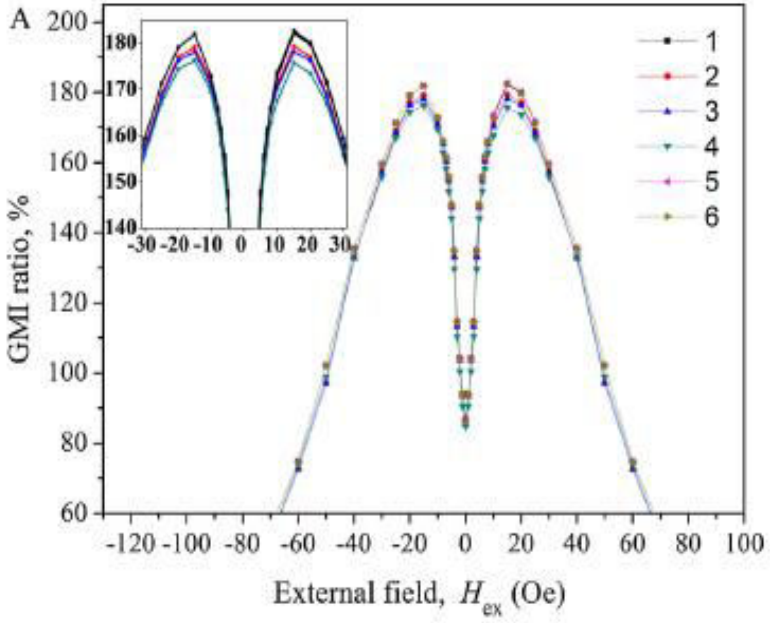


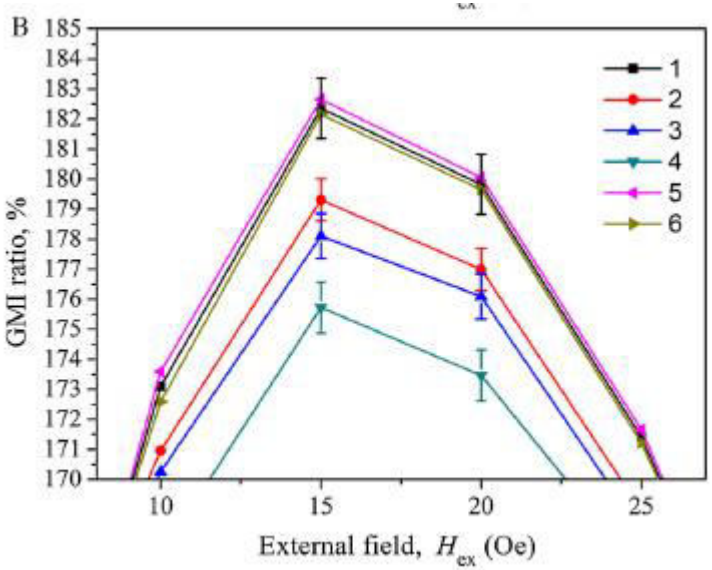

Functionalized magnetic nanoparticles: (A)TEM;(B) SEM



- 血液中胃癌细胞的快速捕获
- 可用于疗效监测
- 检测时间20分钟
- 特异性100%

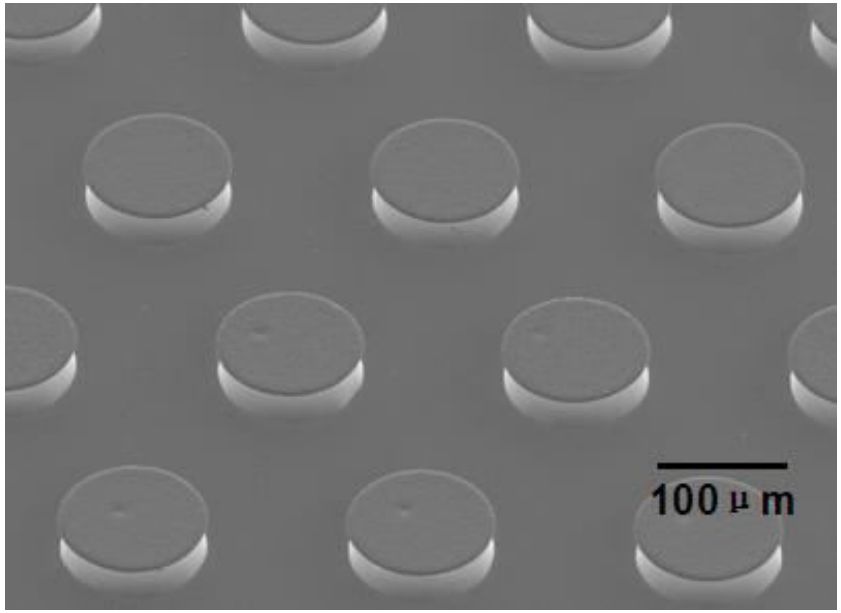


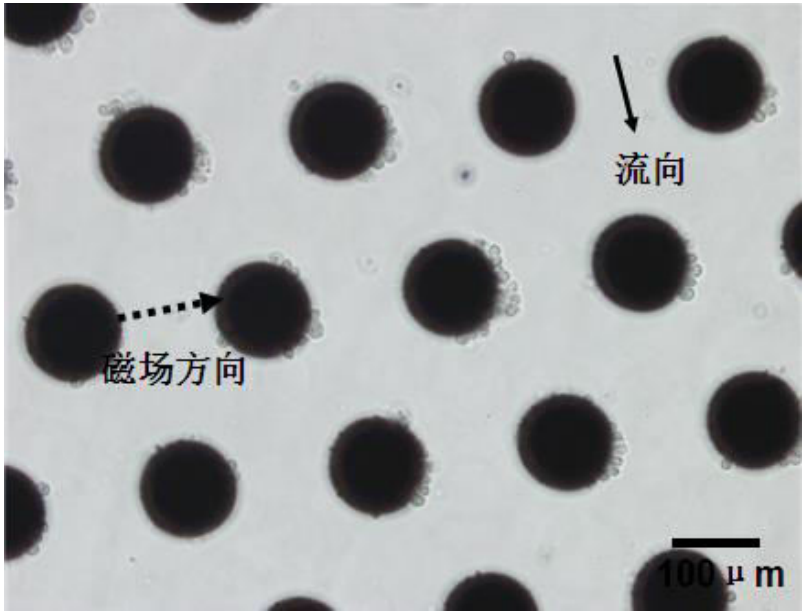




Chen, et al. *Biosensors and Bioelectronics* 2011：6：2435-2442.

# MEMS Capturing Chip based on Magnetic column

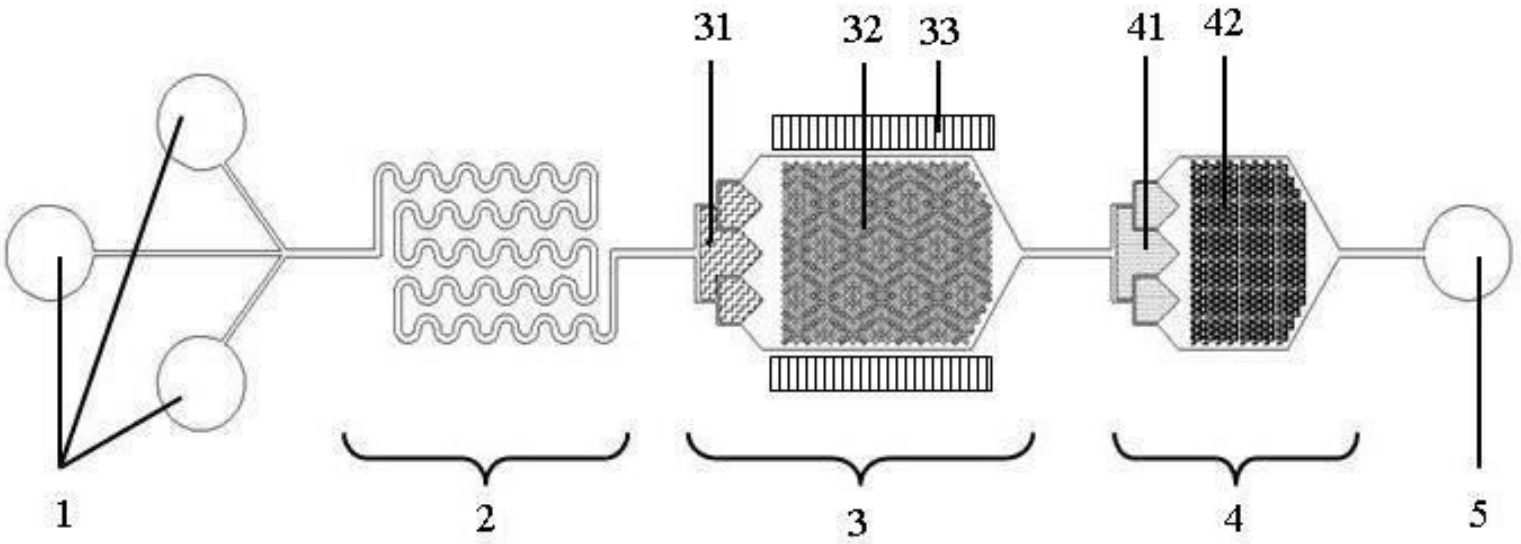



SEM picture of magnetic column




Cancer cell capturing picture

# One rapid isolation and capturing chip for CTC cancer



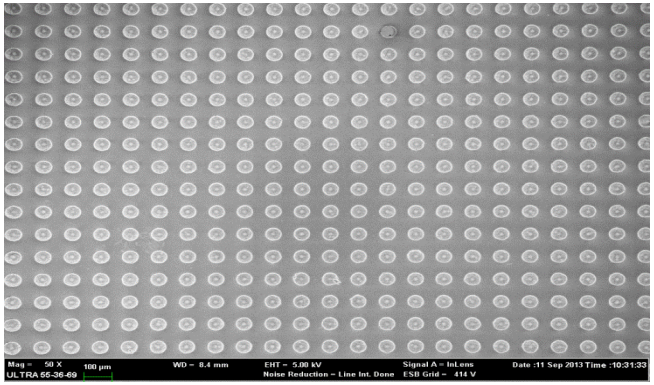

Mixture lysis white cell capturing cancer cell capturing

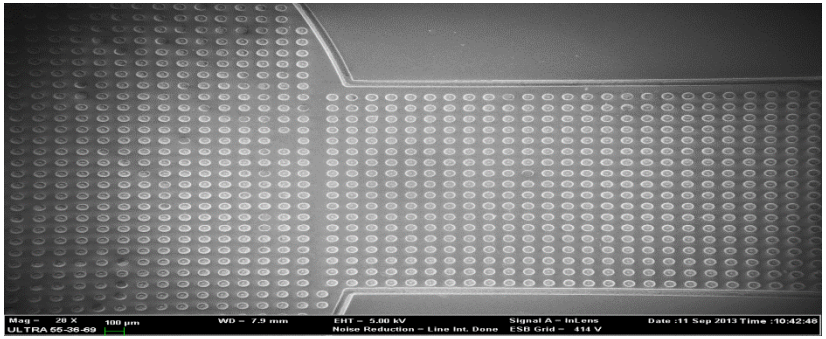
ZL 201110224663.8

# Next Generation of POCT





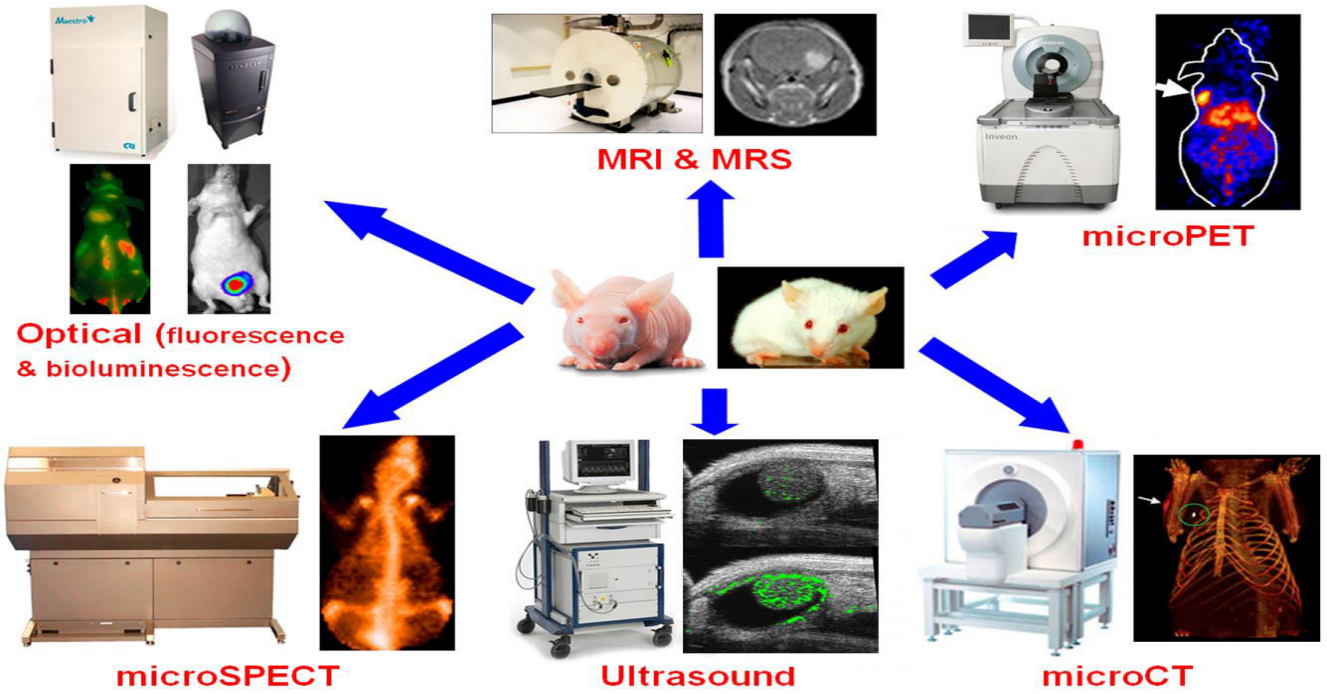

**SEM picture for chip surface**

# Molecular imaging provides one new pathway for new generation of tumor theranostic Technology





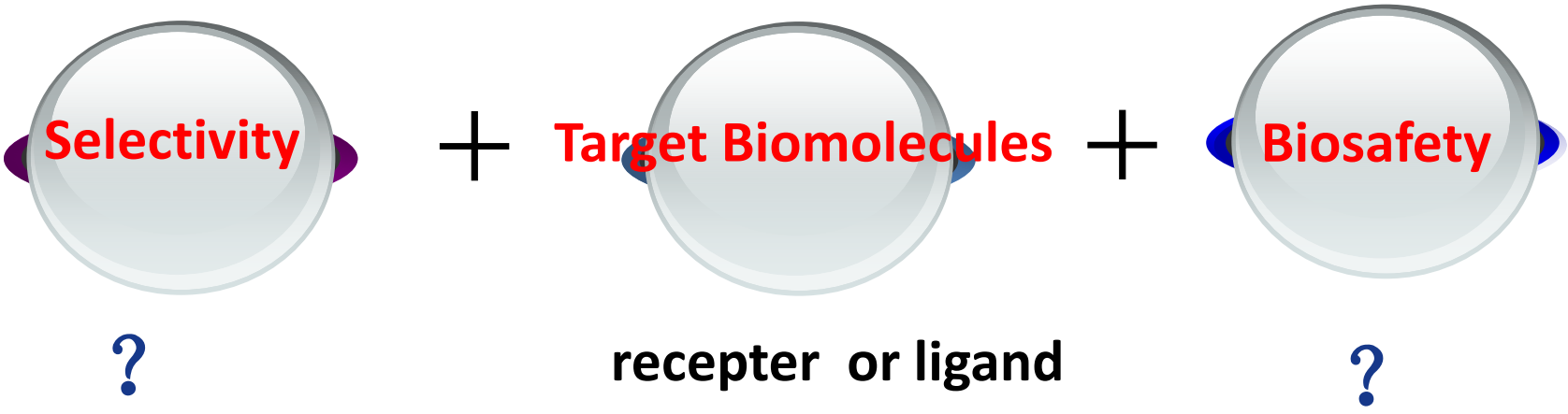

# Molecular Imaging




Multimode molecular imaging

Theranostics, Theragnosis

# How to realize the targeted imaging and therapy of gastric cancer

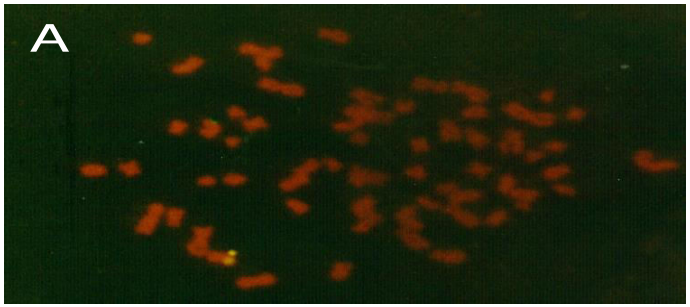



**Successful development of safe and effective nanoprobes for tumor targeting imaging and selective therapy is a great challenge**

# BRCAA1-antibody-conjugated Fluorescent Magnetic Nanoprobes for in vivo targeted imaging of gastric cancer

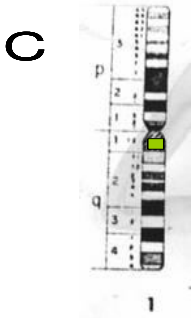
# BRCAA1 Structure and Function

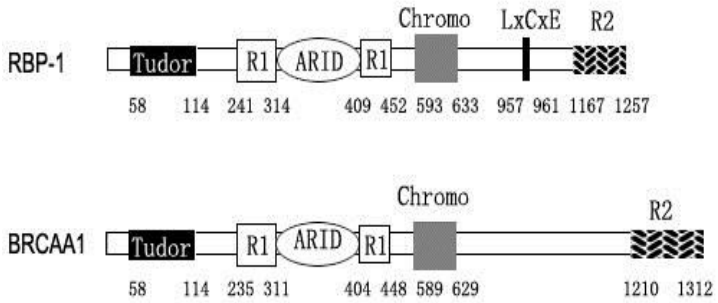
1q42.1-q43. (AF208045)

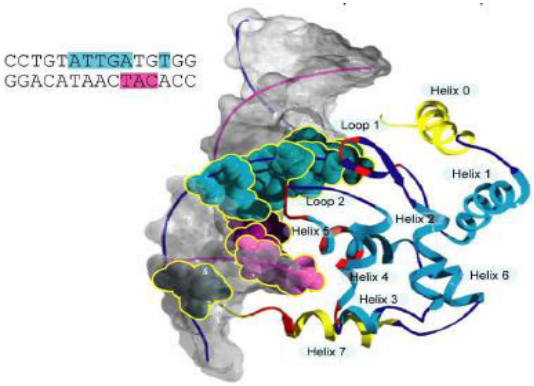








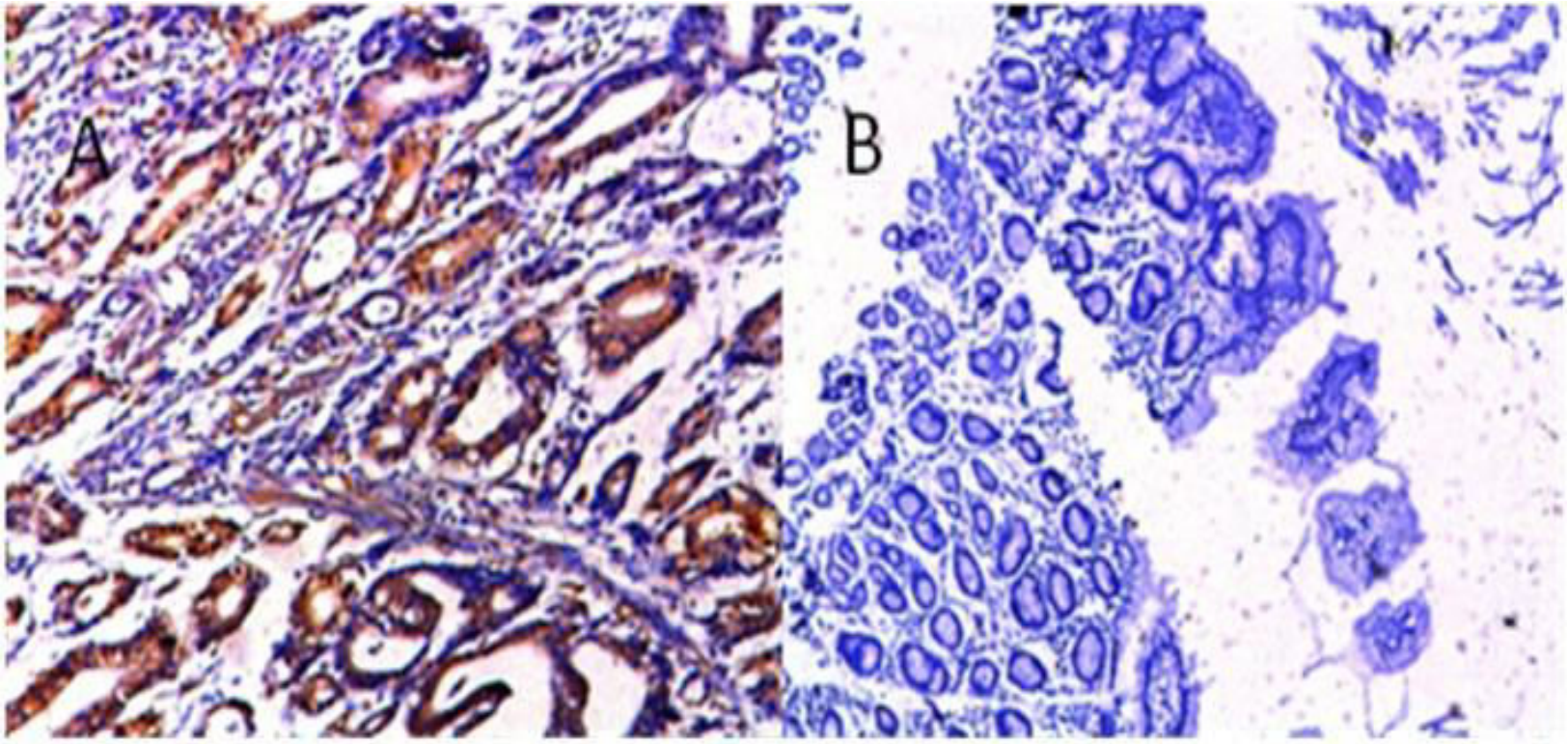




Cui, *et al.* Characterization of BRCAA1 and Its Novel Antigen Epitope Recognization. *Cancer Epidemiology Biomarkers and Prevention* 2004; ***13(7),*** *1136-1145.*

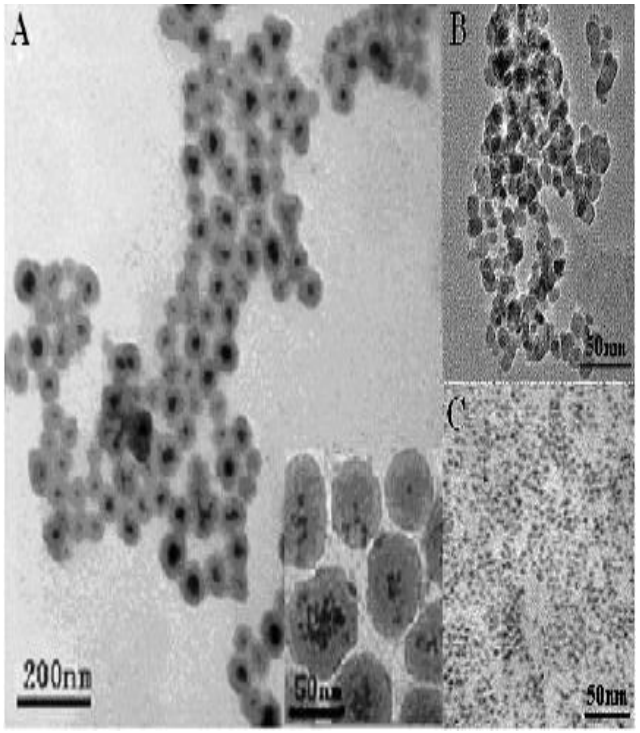
# Titers of BRCAA1 Monoclonal Antibodies in Ascites Fluid Induced by Hybridoma Clone Cells by ELISA

| Clone | Antibody titer* | | | |
|---|---|---|---|---|
| | BRCAA1 (C)-OVA ** | BRCAA1 (C)-BSA ** | BSA ** | OVA ** |
| S-200-5 | 1,024,000 | 1,024,000 | <1,000 | <1,000 |
| S-335-5 | 128,000 | 512,000 | <1,000 | <1,000 |

*The reciprocal of ascites fluid dilution, the first dilution of ascites fluid was 1:1,000. **The antigens were coated on ELISA plate.



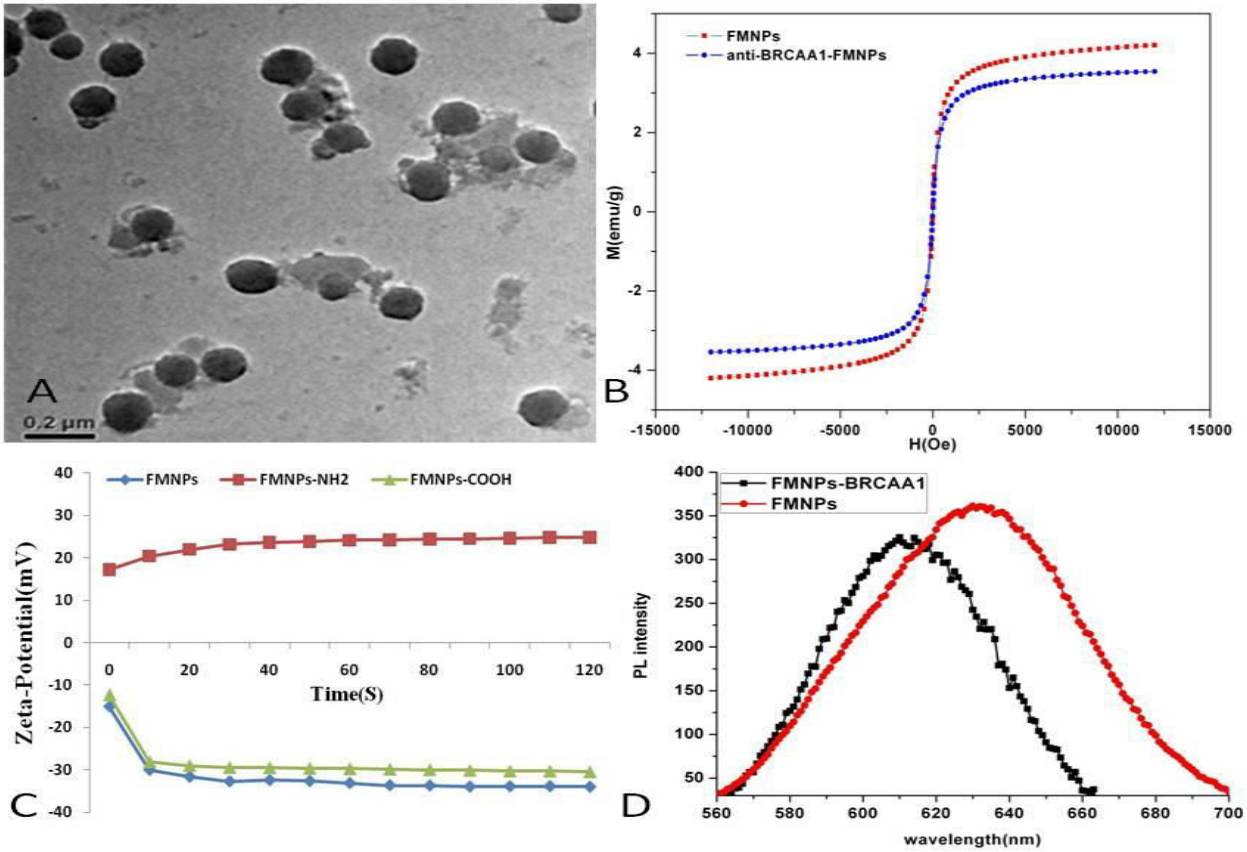

**65% gastric cancer tissues with BRCAA1 over-expression**








**Characterization of Fluorescent Magnetic Nanoparticles (FMNPs)**

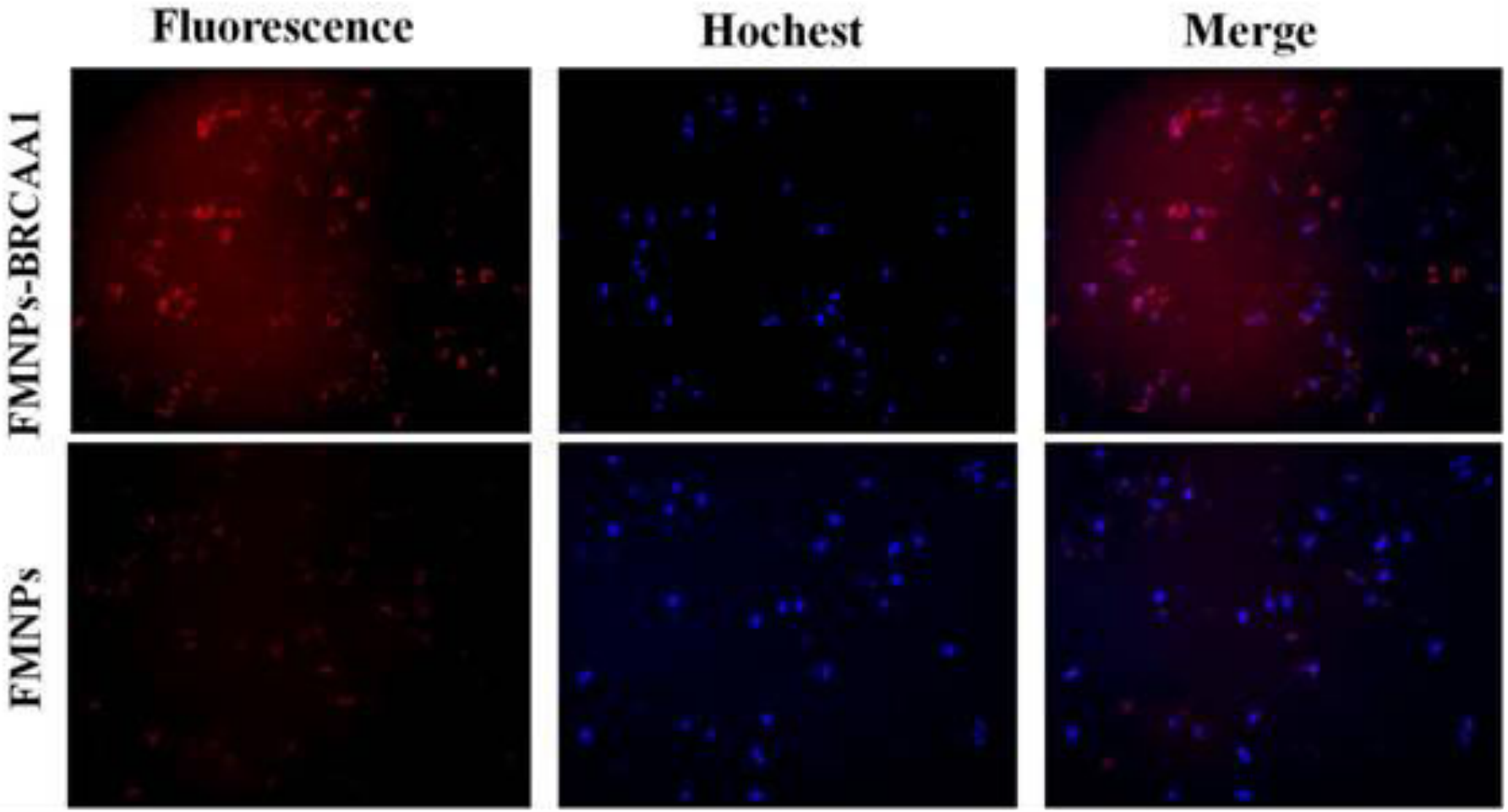


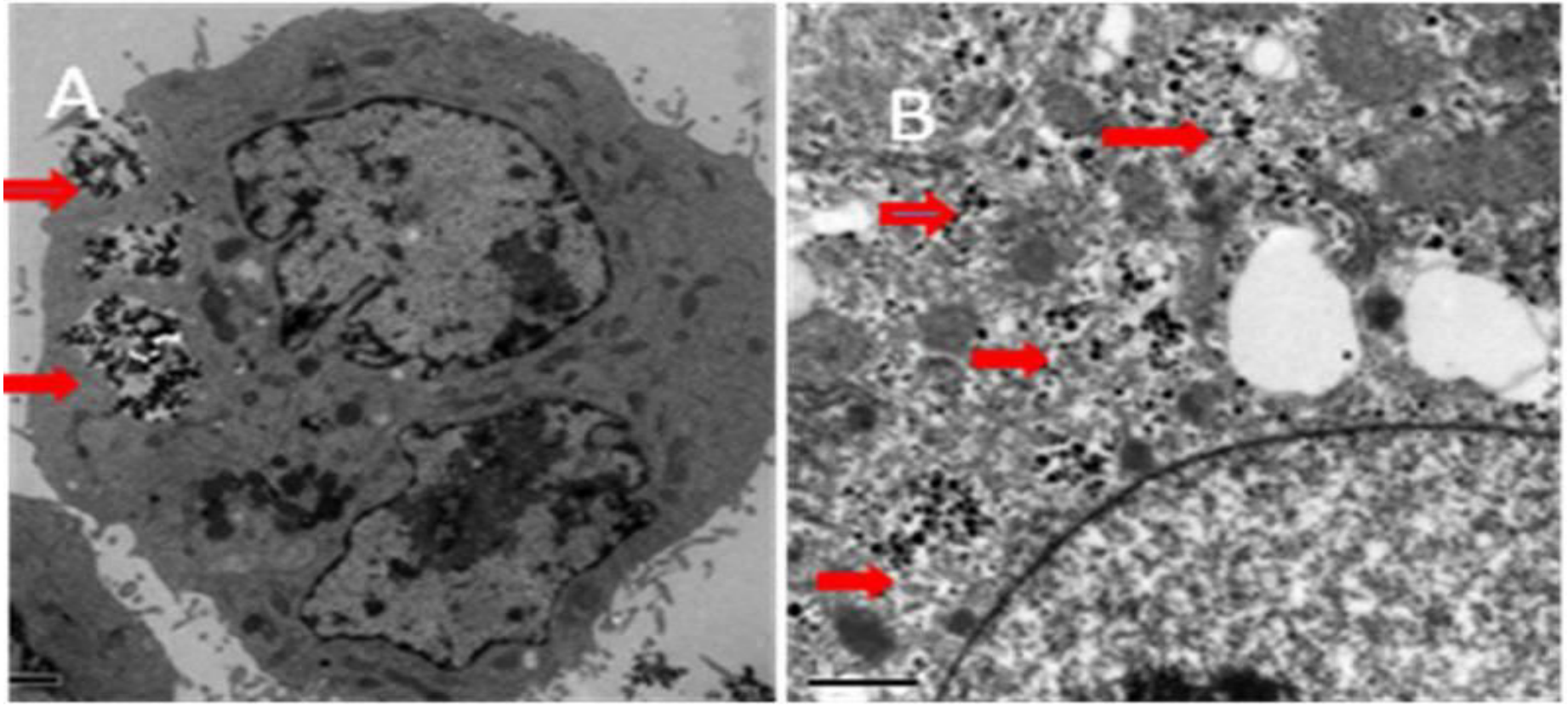

**Characterization of BRCAA1-Monoclonal Antibody-conjugated FMNPs [ BRCAA1-MNPs]**

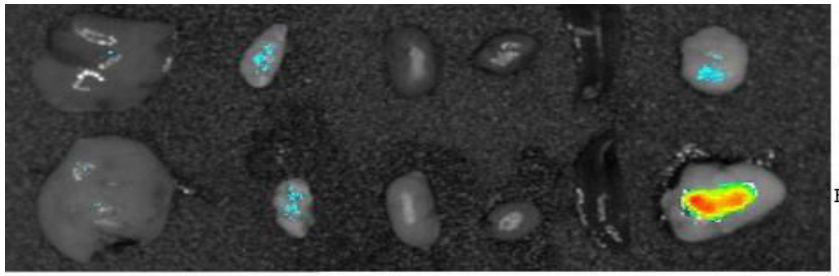
# Coupling rate of FMNPs-BRCAA1 antibody

| | **Total concentration of the anti-BRCAA1 antibody (ng/μL)** | **The concentration of BRCAA1 antibody in residual reaction mixture (ng/μL)** | **Coupling rate (%)** |
|---|---|---|---|
| | 1000.0 | 197.3 | 80.27 |
| | 1000.0 | 191.2 | 80.88 |
| | 1000.0 | 203.0 | 79.70 |

# Nanoprobes for Targeted In Vitro Gastric Cancer Cells



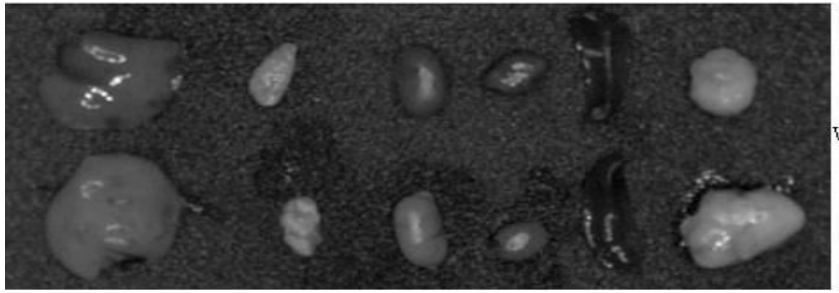

A
B



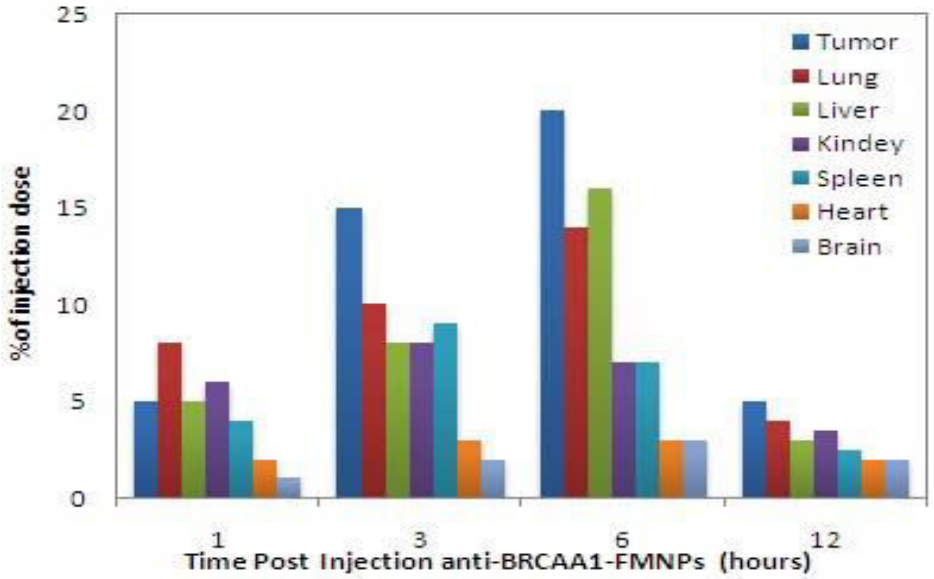
FMNPs Fluorescence imaging (FLI)

FMNPs-BRCAA1 FLI

**Liver lung kidney heart spleen tumor**



White light





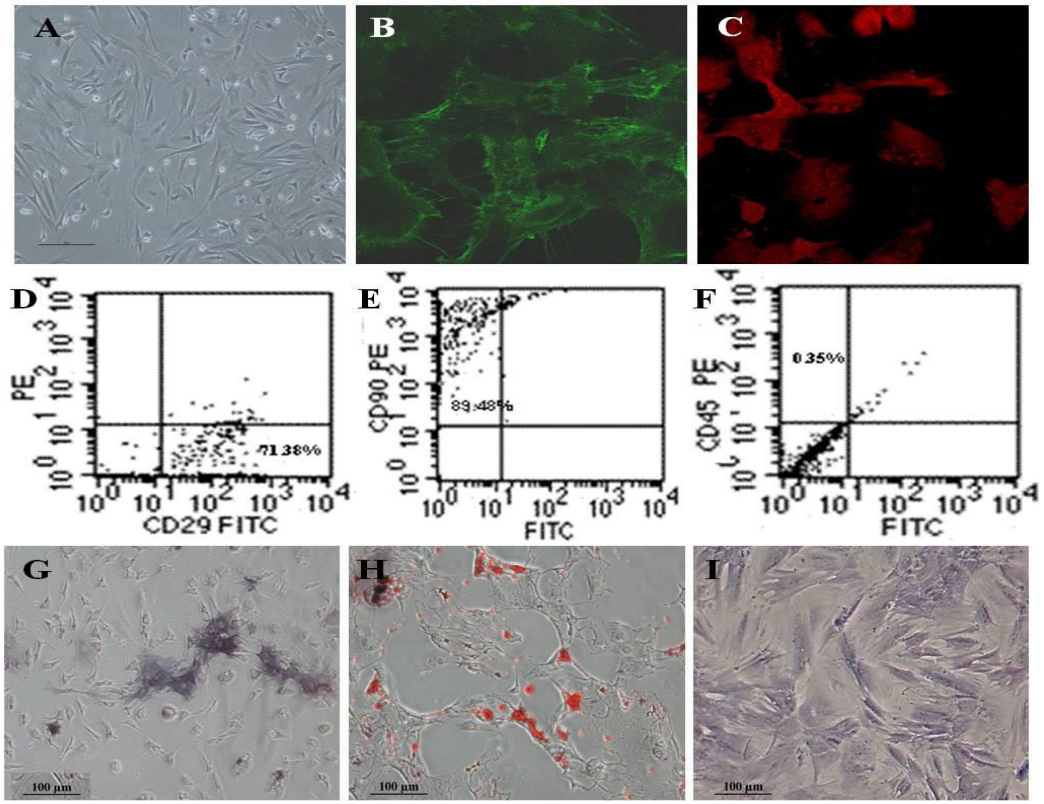

MRI imaging of gastric cancer



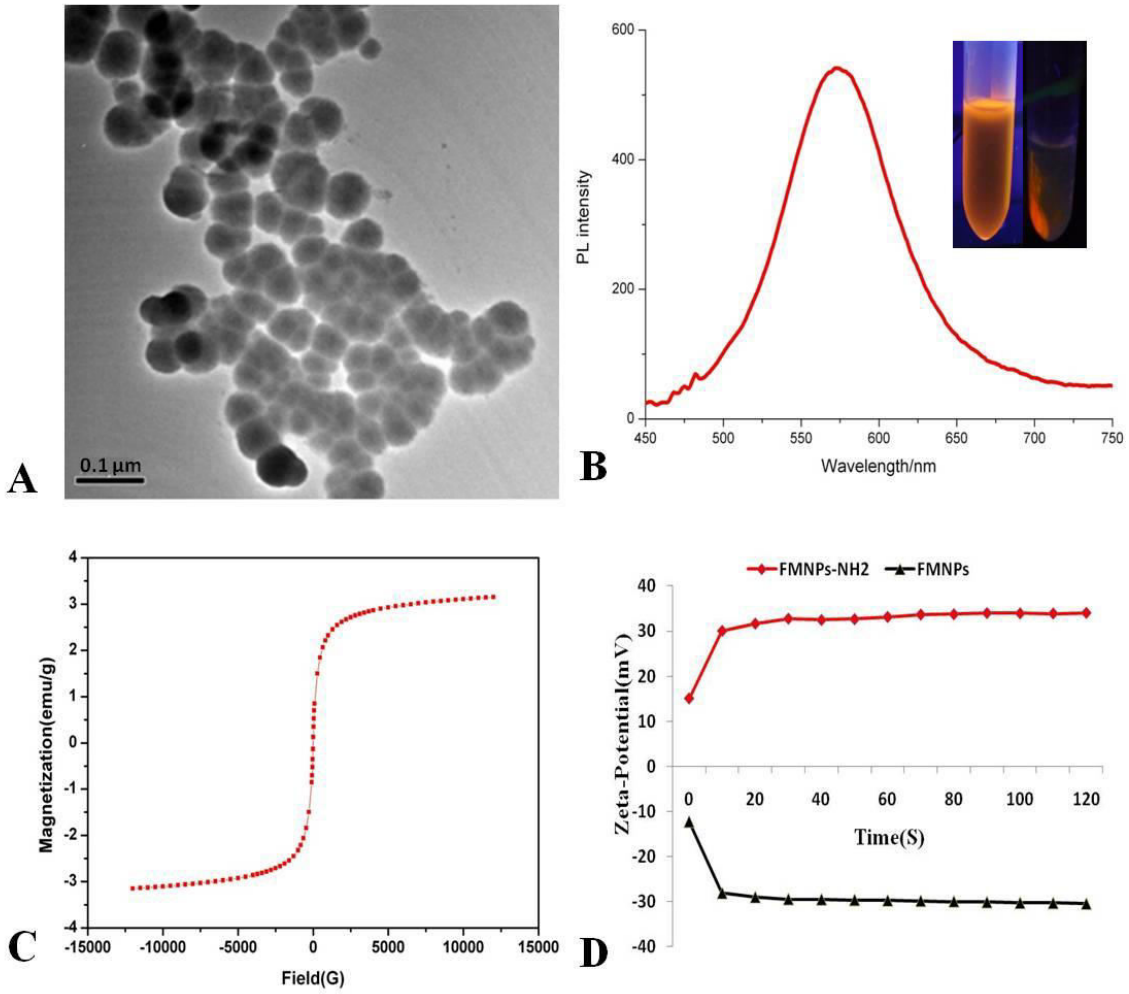



mice model of in situ gastric cancer

# FMNPs-labeled MSCs for Targeted Imaging and Therapy of Gastric Cancer

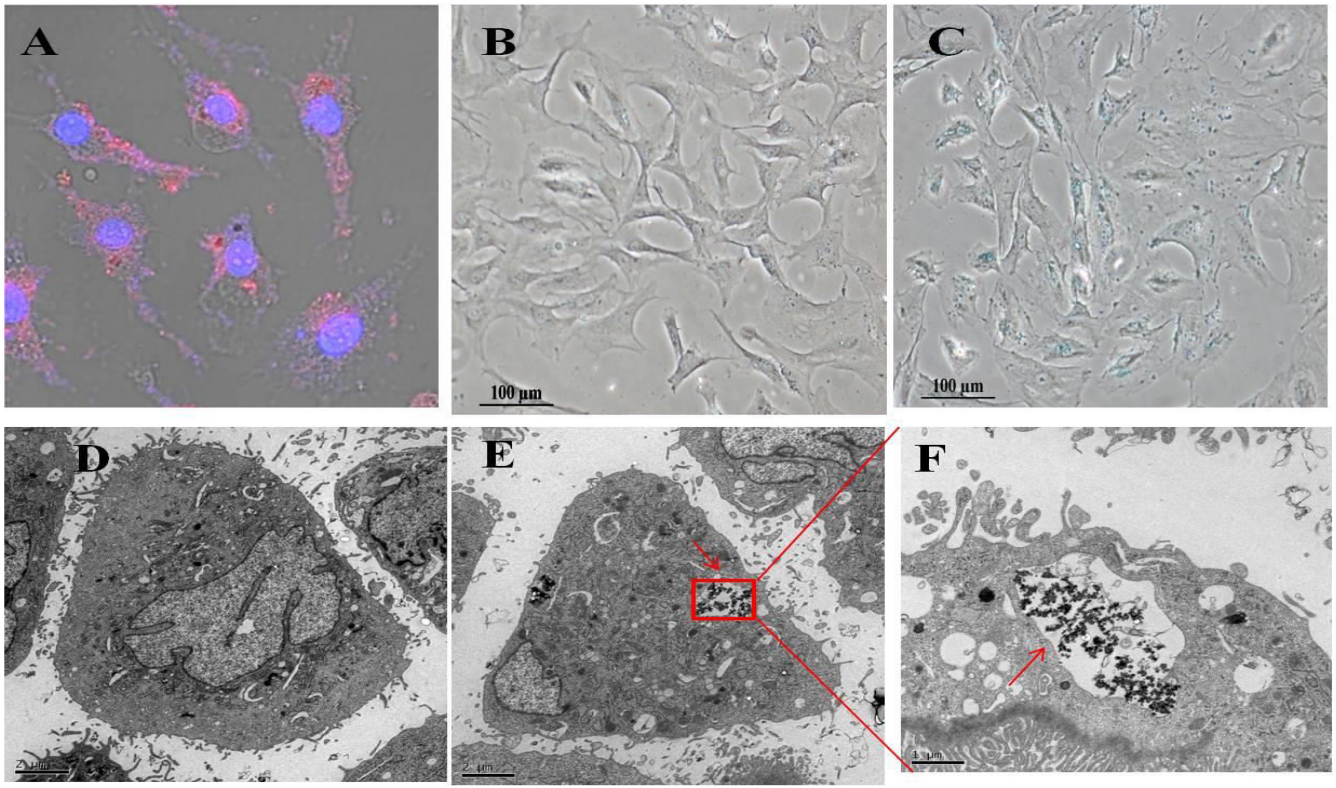



**Morphology and immunophenotypic characterization of MSCs. (**A) The fibroblastic morphology of passage 3 MSCs (Magnification= ×100); (B) MSCs stained with **FITC conjugated CD29 antibody** (200×); (C) MSCs stained with PE conjugated **CD90 antibody** (200×); (D), (E), (F): MSCs analyzed by FACS for the positive expression of **CD29 (D), CD90 (E) and negative expression of CD45** (F); (G) Differentiated osteoblasts tested with **alkaline phosphatase staining** (Magnification= ×100); (H) Differentiated adipocytes characterized by oil red O staining (Magnification= ×100); (I) Differentiated chondrocytes verified **by toluidine blue staining** (Magnification= ×100).

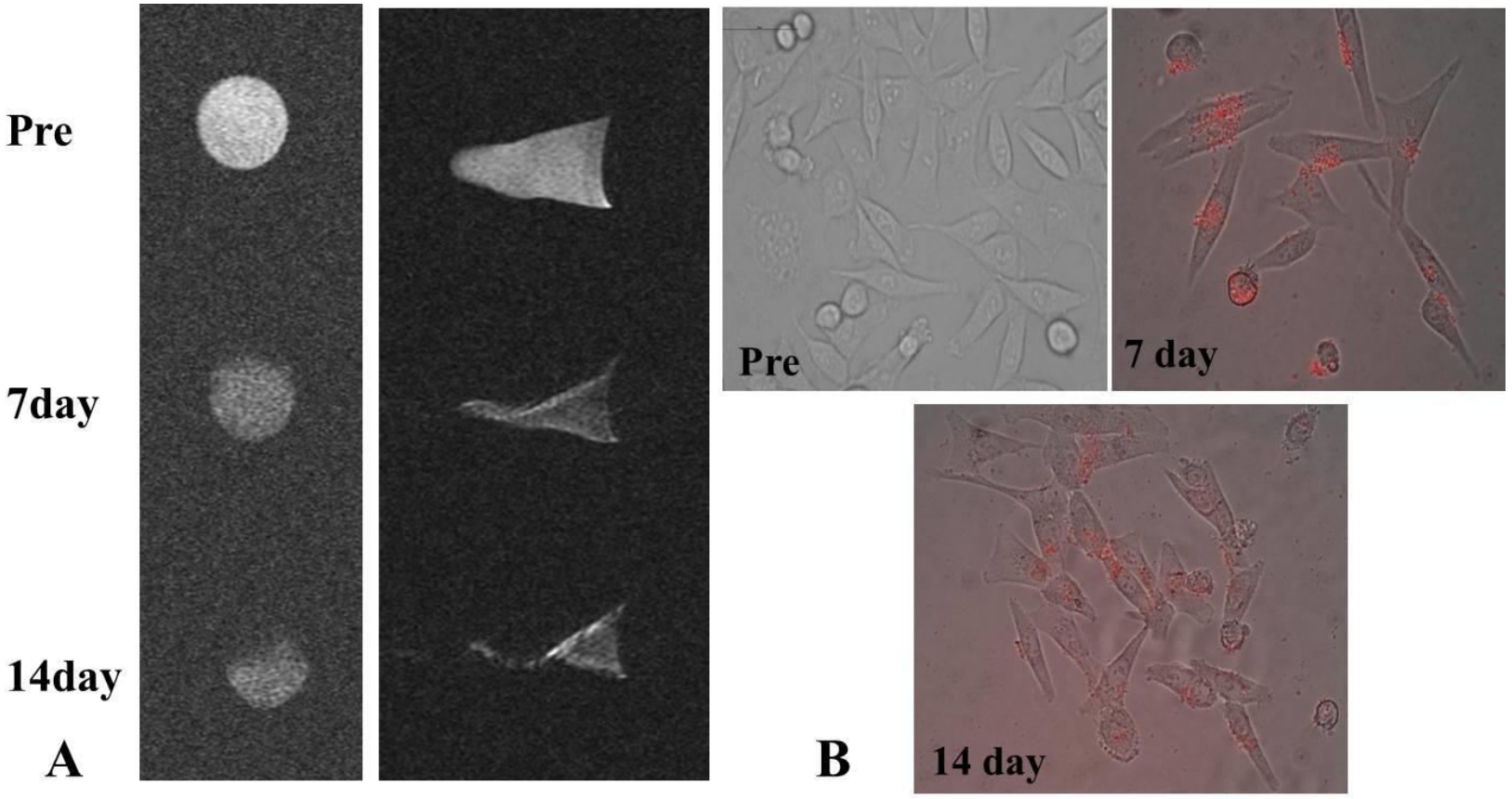



44.8meu/g

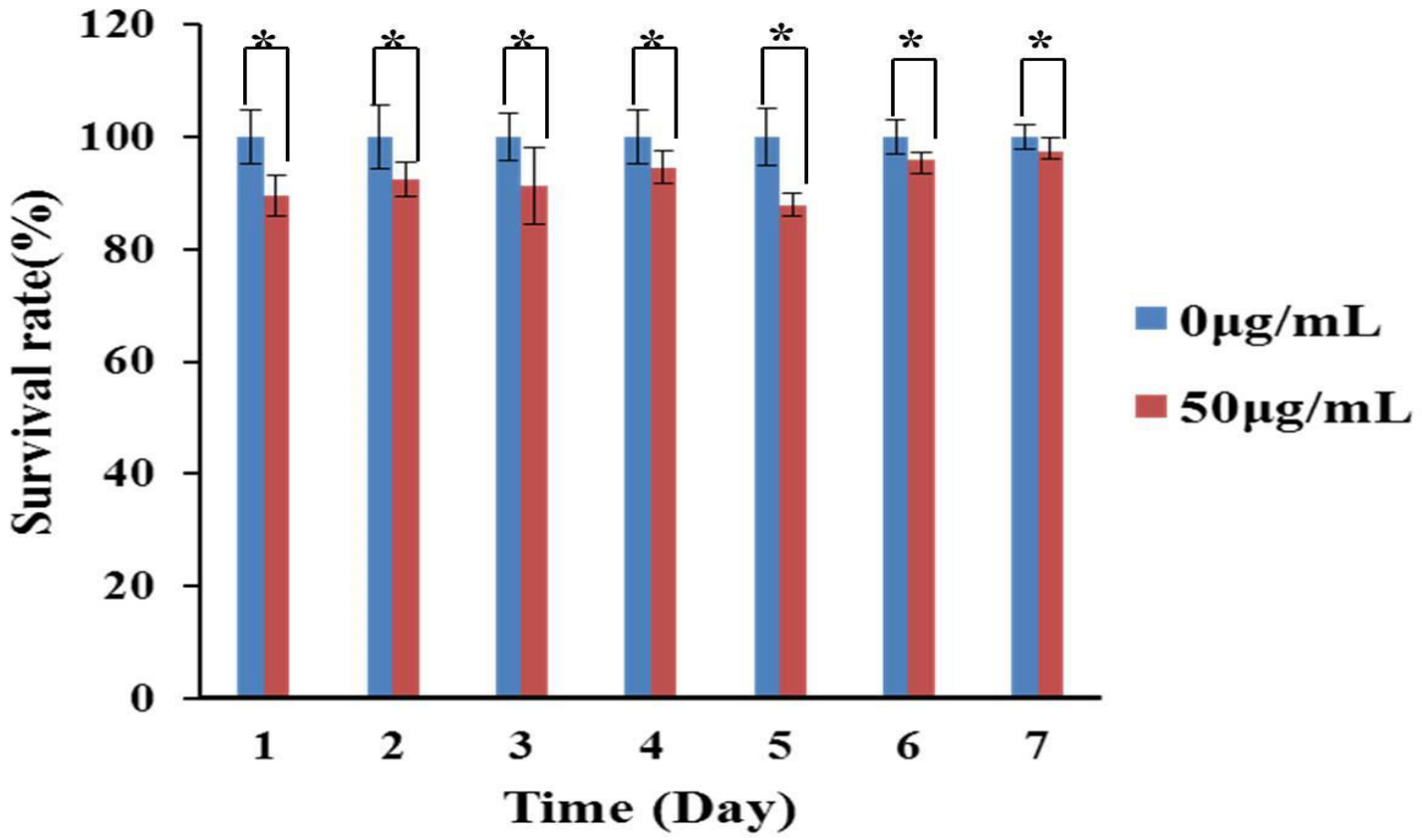
**Characterization of FMNPs. (**A) TEM image of amino-modified FMNPs; (B) PL intensity of amino-modified FMNPs; (C) Magnetic intensity curve of amino-modified FMNPs; (D) Zeta-potential of FMNPs with amino group and Si-O group.




**Evaluation of FMNPs-labeled MSCs.** (A) Cell nucleuses and FMNPs were visible in the MSCs by fluorescent microscope observation (200×); (B) FMNPs-labeled MSCs were detected by using Prussian blue staining(100×); (C) non-labeled MSCs were detected by using Prussian blue staining (100×); (D) The TEM image of non-labeled MSCs; (E) The TEM image of **FMNPs-labeled MSCs** illustrate that amino-modified FMNPs were randomly distributed in the cytoplasm of MSCs (6000×); (F) The magnification image of FMNPs distributed in the cytoplasm of MSCs (12000×).



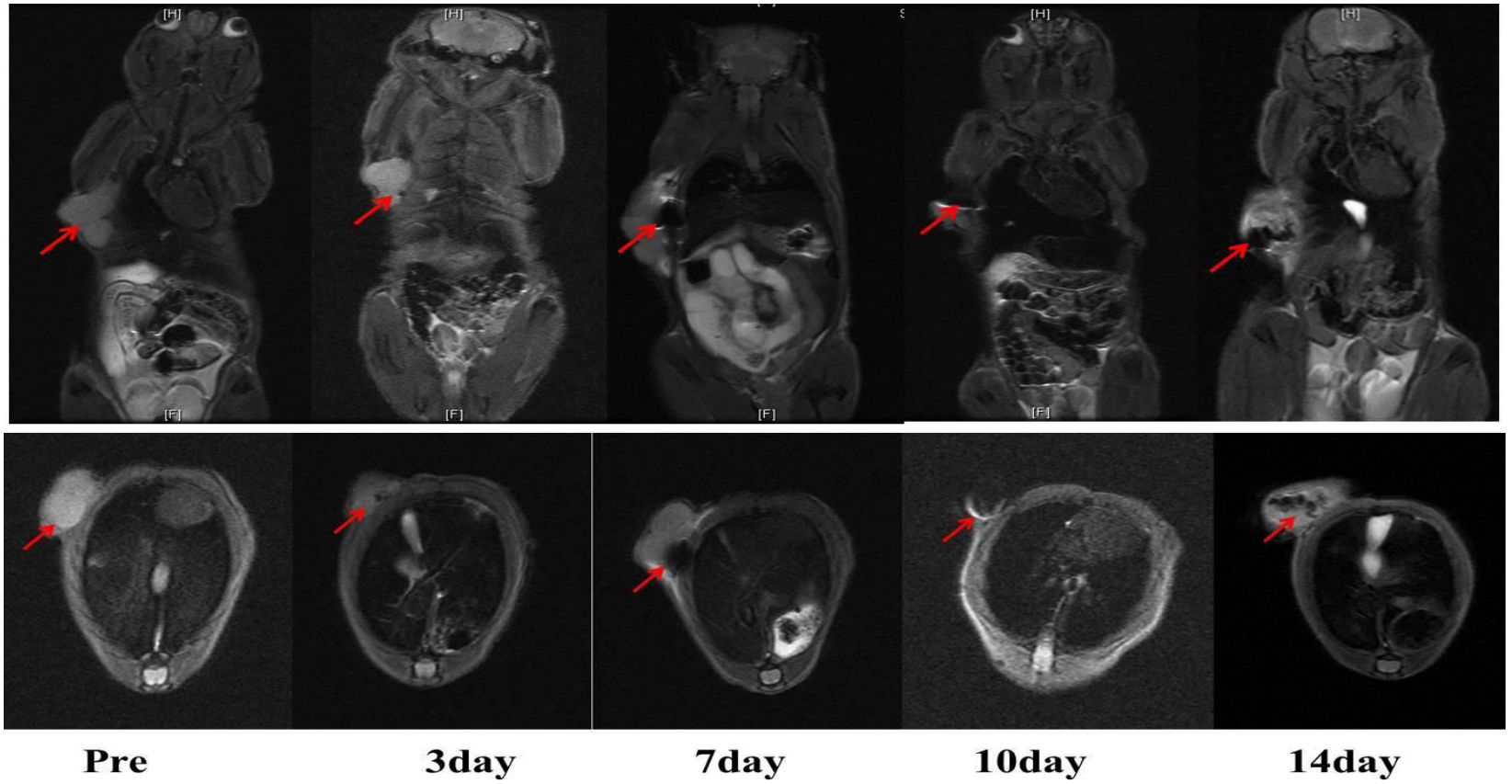

**Labeled stability of the FMMPs-labeled MSCs.** (A) MR imaging of MSCs after being labeled FMNPs 7 and 14 days. (B) Fluorescent microscope images of MSCs after being labeled FMNPs 7 and 14 days (200×).



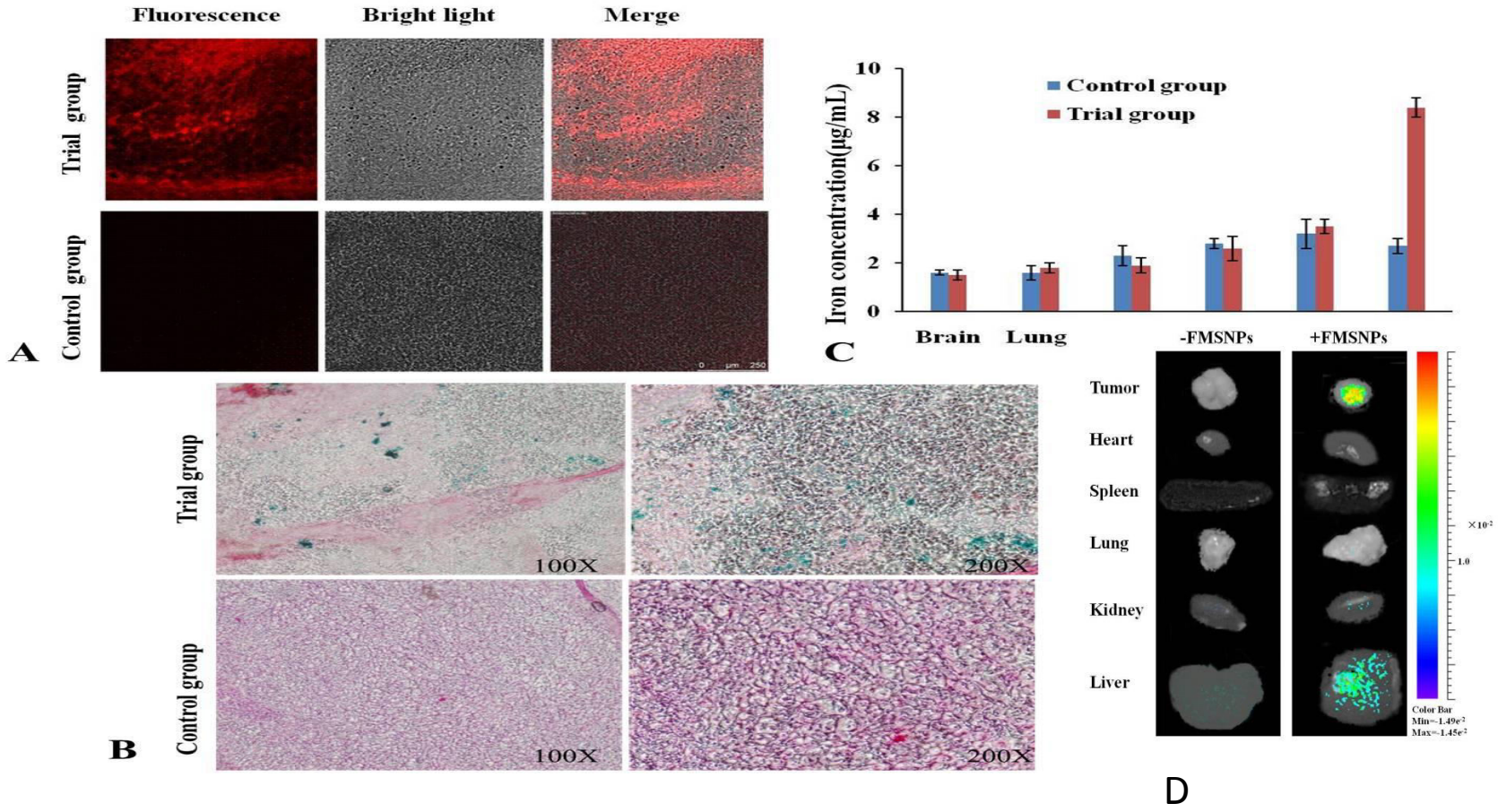

**Effects of amino-modified FMNPs on MSCs.** The survival rates of MSCs after being labeled with FMNPs keep increasing from day 1 to day 7. Mean values ± standard deviation (SD) of independent experiments are shown. Asterisk represents $P < 0.05$.



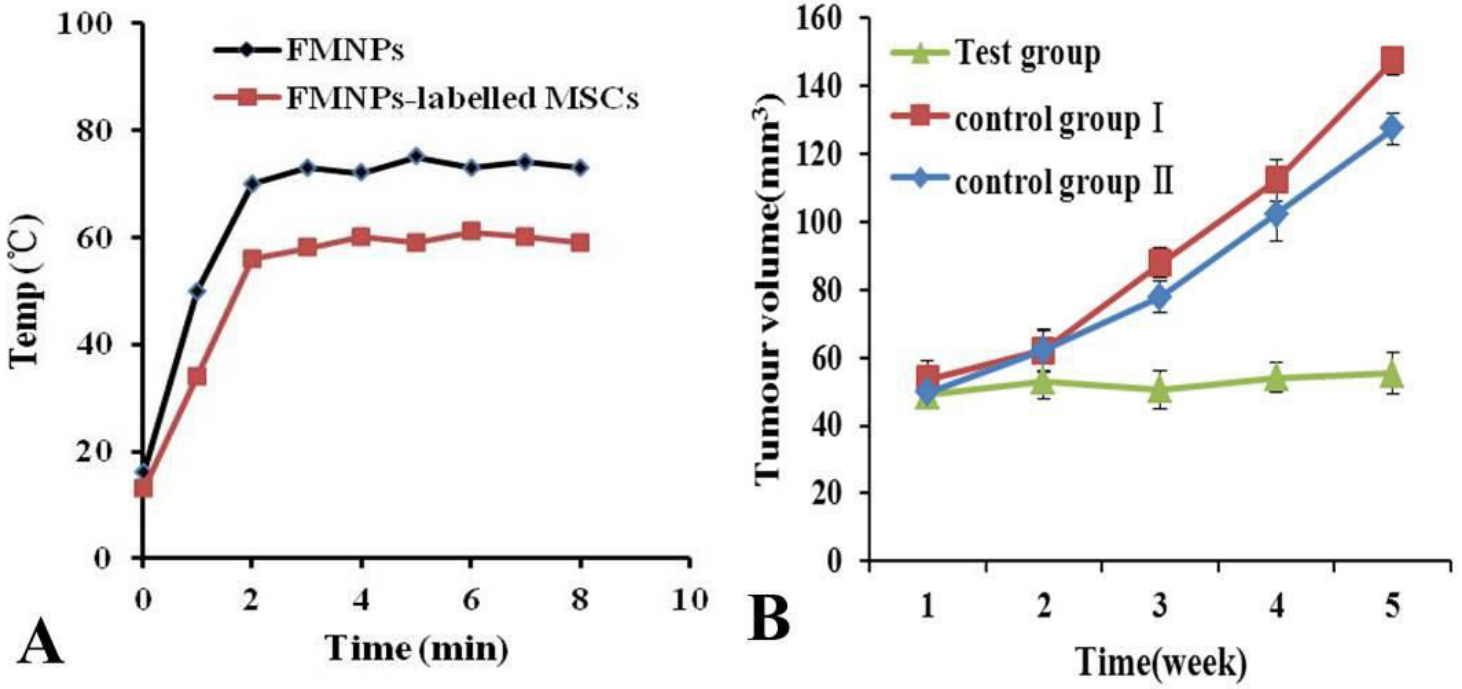

**Fluorescent imaging of FMNPs-labeled MSCs targeting gastric cancer cells *in vivo*.** (A) The *in vivo* fluorescent images show that tumor sites of the mice in test group had fluorescent signals after post-injection **FMNPs-labeled MSCs 7 and 14 days** (right), and tumor sites of the mice in control group had no fluorescent signal **after post-injection FMNPs 7 and 14 days** (left)




MR **imaging of FMNPs-labeled MSCs targeting gastric cancer cells.** The coronal and transected images of MRI show that **MSCs firstly presented in the tumor tissue at 7 days post-injection**, and then gradually accumulated in the tumor tissue and reached **peak value at 14 days post-injection.**

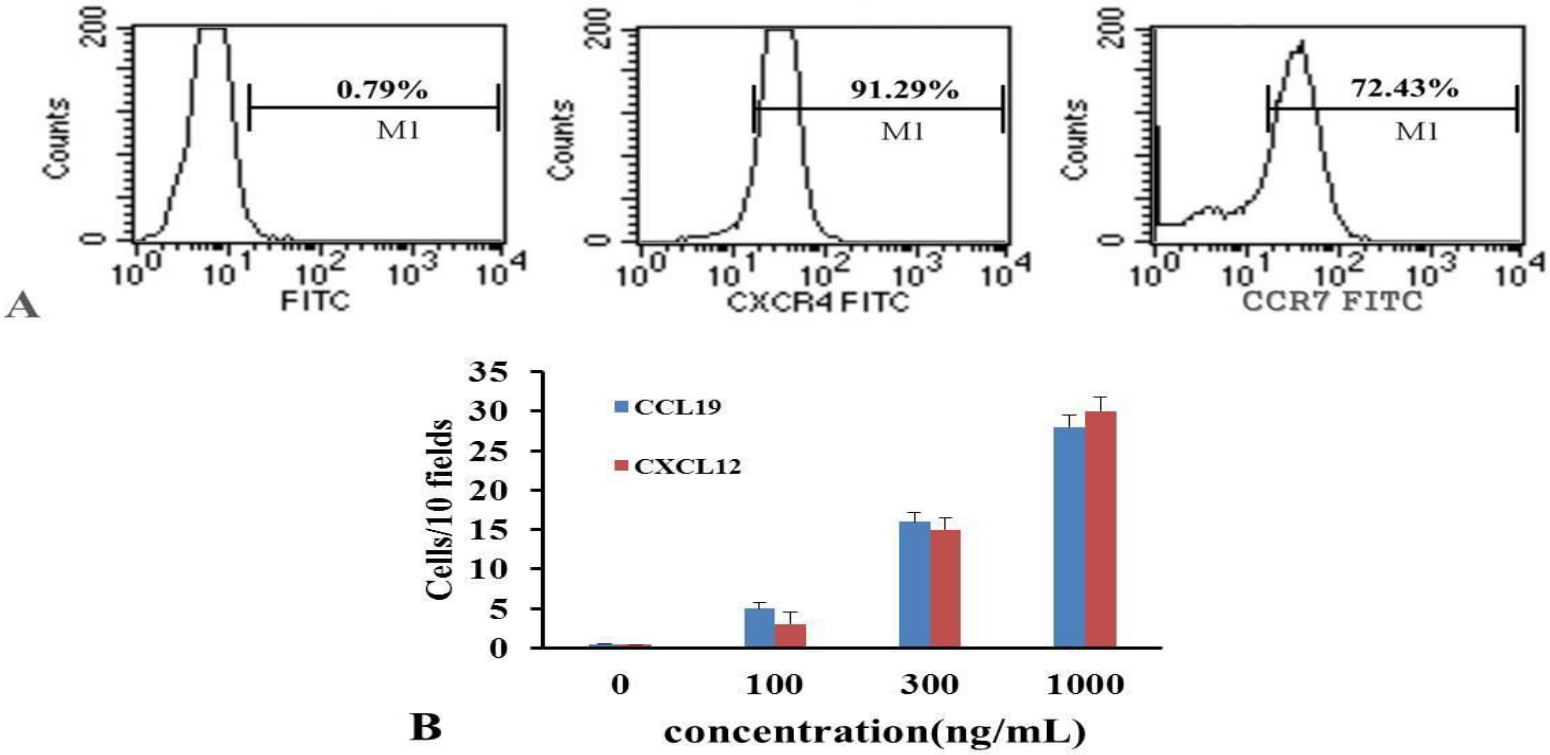



***Ex vivo* analysis of major tissues. (**A) Immunofluorescence staining analysis show that the tumor tissue slices in test group had obvious fluorescent signals, and that in control group had no fluorescent signal; **(**B) Prussian blue staining results show that the tumor tissue slices in test group had blue iron particles, and that in control group had no iron particle; (C) The ICP-MS results show that FMNPs mainly distributed in the tumor tissues of the test group. (D) distribution of labeled MSCs




**Effects of alternating magnetic field on the gastric tumor size. (**A) Time-temperature curve of FMNPs-labeled MSCs under an alternating magnetic field with 63 kHz and 7kA/m； (B) The growth of tumors was inhibited under hyperthermia Therapy.

# Potential Mechanism of MSCs Targeted Tumor




**Analysis of chemokine receptors and chemotaxis**

(A) The expressions of **CXCR4 and CCR7** on MSCs were determined by FACs

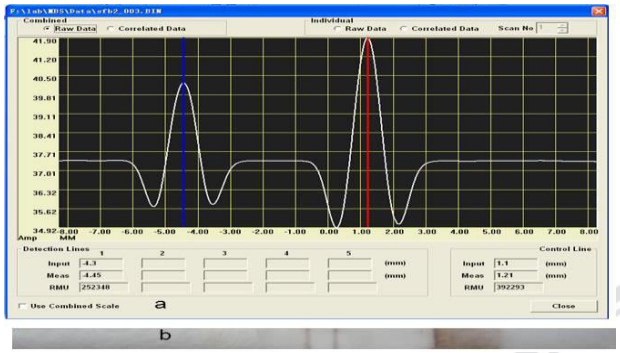
(B) The migration of MSCs to different concentrations of **CXCL12 and CCL19** was evaluated by chemotaxis assay. [13.2±1.8 ng/mL, 5.5±0.7 ng/mL, ]

**CCL19/CCR7 and CXCL12/CXCR4 axis loops may involve in MSCs motion.**

# Strip for quick detection of biomarkers

- **Magnetic or QDs labeling based Strips**





中华人民共和国
PEOPLE'S REPUBLIC OF CHINA
医疗器械注册证
REGISTRATION CERTIFICATE FOR MEDICAL DEVICE
苏食药监械（准）字 2011 第 2400762 号
苏州康立达纳米生物工程有限公司：
你单位生产的生物免疫层析芯片检测仪，经审查，符合医疗器械产品市场准入规定，准许注册。自批准之日起有效期四年。
特此证明。
江苏省食品药品监督管理局
二〇一一年八月八日

- Qualtive, quantitative detection ； sensitivity: 5pg/ml;
- Specificity : 98%





Hu, et al. Chem. Commun. 2010; 46: 3866-3868.:[IF5.787]

Gao, et al. J. Mater. Chem. 2011; 2011, 13, 1782-1785

Zhang, et al. J. Biomed. Nanotechnol. 2011; 7; 776-781.

Yang, et al. Nanoscale Res. Lett. 2009; 4: 1469-1474.

Yang, et al. Nanoscale Res. Lett. 2010; 5: 875-881.

# Acknowledgement

**This work was supported by National 973 project (2010CB933900), 863 Project (No.2007AA022004), National Natural Scientific Fund (No. 81225010 and 20771075), and Shanghai Nano-Project (1052nm041000), and International Cooperation Budget of Waseda university .**



# Thanks for your attention!

# Let Us Meet Again

We welcome you all to our future conferences of OMICS Group International

Please Visit:

www.omicsgroup.com

www.conferenceseries.com

www.pharmaceuticalconferences.com